Posttranscriptional regulation of ribosomal and multiresistance genes by the bacterial leader peptide peTrpL

Hendrik Melior[1], Siqi Li[1], Maximilian Stötzel[1], Konrad U. Förstner[2], Sandra Maaß[3], Rubina Schütz[1], Saina Azarderakhsh[1], Susanne Barth-Weber[1], Aleksei Shevkoplias[4], Kathrin Baumgardt[1], Zoe Chervontseva[5,6], John Ziebuhr[7], Christian H. Ahrens[8], Elena Evguenieva-Hackenberg[1*]

[1] Institute of Microbiology and Molecular Biology, University of Giessen, Germany

[2] ZB MED - Information Center for Life Sciences, University of Cologne, Germany

[3] Institute of Microbiology, University of Greifswald, Germany

[4] Laboratory for Marine Benthic Ecology and Hydrobiology, Anichkov Lyceum, St. Petersburg, Russia

[5] Kharkevich Institute for Information Transmission Problems RAS, Moscow, Russia

[6] Center for Life Sciences, Skolkovo Institute of Technology, Moscow, Russia

[7] Institute of Medical Virology, University of Giessen, Germany

[8] Agroscope & SIB Swiss Institute of Bioinformatics, Wädenswil, Switzerland

* Corresponding Author / Leader contact

Email: Elena.Evguenieva-Hackenberg@mikro.bio.uni-giessen.de

Summary

Ribosome-mediated transcription attenuation in bacteria is an important regulatory mechanism that is controlled by the translation of a short upstream ORF (uORF). Efficient uORF translation causes transcription termination downstream of the uORF. The resulting leader peptide and small attenuator RNA are generally considered nonfunctional. Here, we show that, upon exposure to translation-inhibiting antibiotics, the leader peptide peTrpL (14 aa) of a *Sinorhizobium meliloti* tryptophan (Trp) biosynthesis operon acts together with its cognate attenuator RNA rnTrpL to destabilize *rplUrpmA* mRNA which encodes ribosomal proteins. Under these conditions, rnTrpL is produced independently of Trp availability by transcription termination at the attenuator. In addition, the peTrpL peptide has an rnTrpL-independent function in a pathway that is induced by effectors of the TetR-type repressor SmeR. The peTrpL was found to destabilize *smeR* mRNA, resulting in increased multidrug efflux and multiresistance. The surprising role of peTrpL in antibiotic-triggered posttranscriptional regulation is conserved in other bacteria.

Introduction

Short upstream open reading frames (uORFs) in mRNA leaders are widespread *cis*-elements of posttranscriptional gene regulation (Andrews and Rothnagel, 2014; Dar and Sorek, 2017). Functions of eukaryotic uORFs and/or their translation products include regulation of mRNA stability or translation initiation of the downstream (main) ORF in *cis* (Cabrera-Quio et al., 2016). Although approximately half of all eukaryotic mRNAs contain uORFs, only few examples for uORFs encoding *trans*-acting peptides have been reported (Cabrera-Quio et al., 2016; Kereszt et al., 2018). Since in bacteria, transcription and translation can be coupled, bacterial uORFs are mainly known for their ability to regulate transcription termination by ribosome-dependent attenuation (Yanofsky, 1981). Additionally, bacterial uORF-containing RNA leaders and/or the small proteins (called leader peptides) encoded by these RNA leaders can regulate in *cis* the translation of downstream ORFs (Lovett and Rogers, 1996; Park et al., 2017). However, specific functions of the bacterial leader peptides in *trans* have not been reported.

Ribosome-dependent attenuation of transcription termination is best studied in *Escherichia coli*, where the Trp biosynthesis genes *trpEDCBA* are co-transcribed (Yanofski, 1981). The 5' mRNA leader harbors the uORF *trpL*, which contains several consecutive Trp codons. Under conditions of Trp insufficiency, ribosome pausing at the Trp codons prevents the formation of a transcriptional terminator downstream of the uORF, thus resulting in co-transcription of *trpL* with the structural *trp* genes. In contrast, if enough Trp is available, fast translation of the Trp codons causes transcription termination between *trpL* and *trpE* and, as a result, a small attenuator RNA containing the short ORF (sORF) *trpL* is released. Generally, the released attenuator RNA and its encoded leader peptide are considered non-functional.

In many bacteria including the plant symbiont *Sinorhizobium meliloti*, the *trp* genes are organized in several operons, only one of which is regulated by attenuation (Merino et al., 2008). In *S. meliloti*, the *trp* attenuator is located upstream of *trpE(G)* (Fig. 1A), which is transcribed separately from *trpDC* and *trpFBA* (Bae and Crawford, 1990). We recently found that, in *S. meliloti*, the released *trpL*-containing attenuator RNA destabilizes the *trpDC* mRNA in *trans* (Melior et al., 2019). This small RNA (sRNA) was named rnTrpL (synonym RcsR1; Baumgardt et al., 2016). Previously, rnTrpL was predicted to base-pair with several additional mRNAs including *sinI* (encoding an autoinducer synthase), which was subsequently confirmed to be another direct target of rnTrpL (Baumgardt et al., 2016).

Transcription attenuators are prevalent in amino acid (aa) biosynthesis operons of gram-negative bacteria (Vitreschak et al., 2004). Recently, they were also found to regulate antibiotic resistance operons of gram-positive bacteria: upon exposure of *Bacillus* or *Listeria* to translation-inhibiting antibiotics, ribosome stalling at uORFs prevents termination of transcription, thus inducing the expression of downstream resistance genes (Dar et al., 2016). The widespread occurrence and high synteny conservation of attenuator uORFs raises the question of whether some of their leader peptides may have gained independent functions in *trans* during evolution. This hypothesis is inspired by the increasing evidence for functional small proteins encoded by sORFs shorter than 50 codons, which often are missing in current genome annotations (Storz et al., 2014). For example, in *Drosophila*, small proteins of between 11 and 32 aa in length regulate cell morphogenesis (Kondo et

al., 2007) and, in *Bacillus subtilis*, the basic 29-aa protein FbpC was proposed to act as an RNA chaperone (Gaballa et al., 2008), whereas, in *E. coli,* the 31-aa protein MgtS was shown to interact with two different proteins and regulate Mg^{2+} homeostasis (Yin et al., 2018). These examples underline why sORF-encoded proteins have become an important research field (Andrews and Rothnagel, 2014; Storz et al., 2014; Omasits et al., 2017; Weaver et al., 2019).

Here, we analyzed a predicted interaction between mRNA *rplUrpmA* and the attenuator sRNA rnTrpL, focusing on the sORF *trpL*. Surprisingly, we found that both the 14-aa leader peptide peTrpL and the sRNA rnTrpL are required for posttranscriptional downregulation of *rplUrpmA* upon exposure to translation-inhibiting antibiotics. Moreover, we found that peTrpL has an rnTrpL-independent role in the regulation of the major multidrug efflux pump operon *smeABR* in *S. meliloti*. Evidence for the conservation of both functions in other bacteria is presented.

Results

The attenuator sRNA rnTrpL requires the leader peptide peTrpL and tetracycline for down-regulation of *rplUrpmA* mRNA

The *rplUrpmA* operon encodes the ribosomal proteins L21 and L27 and is one of the previously predicted but not yet experimentally verified targets of the sRNA rnTrpL (Baumgardt et al., 2016). To test this prediction, rnTrpL and mutated variants were constitutively overproduced from the tetracycline (Tc) resistance-conferring plasmid pRK-rnTrpL (Fig. S1) in strain *S. meliloti* 2011, and *rplUrpmA* mRNA levels were analyzed. Our preliminary data suggested that rnTrpL, peTrpL and Tc all play roles in *rplUrpmA* regulation (Fig. S2).

For further analyses, we used plasmids pSRKGm-peTrpL and pSRKGm-rnTrpL, which allow for IPTG-inducible production of peTrpL and a rnTrpL variant named lacZ'-rnTrpL, respectively, and confer gentamycin (Gm) resistance (Fig. S1). Cultures of *S. meliloti* 2011 harboring either pSRKGm-peTrpL or pSRKGm-rnTrpL were grown in parallel with two-plasmid cultures that additionally contained the empty plasmid pRK4352, which conferred Tc resistance. IPTG was added for 10 min or for 4 h respectively, and changes in the *rpmA* level were analyzed. In the presence of Tc (and pRK4352), the *rpmA* levels of both rnTrpL- and peTrpL-overproducing strains were decreased at 10 min post induction (p. i.) (Fig. 1B). Interestingly, at 4 h p. i., *rpmA* levels were found to be increased. This increase was similar to the increase observed upon constitutive rnTrpL overproduction using pRK-rnTrpL (see left bar C in Fig. 1B; see also Fig. S2). Notably, in all cultures without Tc (and without pRK4352), no change in the *rpmA* levels was observed (Fig. 1B). This suggested that (i) a short-term (10-min) overproduction of the leader peptide peTrpL in strain 2011 is sufficient to cause a decrease of cellular *rpmA* mRNA levels, while a long-term overproduction (4 h after IPTG addition or upon constitutive overproduction) causes an increase and (ii) these effects may be dependent on Tc.

Next, we analyzed the short-term effects in a *ΔtrpL* background. Strain 2011*ΔtrpL* (pSRKGm-rnTrpL, pRK4352) was grown in medium containing Tc and Gm. 10 min p. i. of lacZ'-rnTrpL (and of peTrpL encoded by this sRNA), the *rpmA* level was decreased like in strain 2011 that still harbored the

chromosomal *trpL* gene (compare Fig. 1C to Fig. 1B). Interestingly, if 2011*ΔtrpL* (pSRKGm-peTrpL, pRK4352) was used (i.e., a *ΔtrpL* strain that only produces peTrpL upon induction), no significant change in the *rpmA* level was observed (Fig. 1C), suggesting that the negative effect on *rpmA* required the presence of both the peptide and the sRNA. To test this, we used two plasmids, each one of them conferring either the sRNA (pRK-rnTrpL-AU1,2UA; see Fig. S2) or the peptide (pSRKGm-peTrpL) function only. A decrease of the *rpmA* level was detected only if both the sRNA and the peptide were produced (Fig. 1D), providing evidence that both peTrpL and rnTrpL are required to downregulate *rplUrpmA*.

To investigate a possible involvement of Tc in the regulation of *rplUrpmA* by rnTrpL and peTrpL, cells of strain 2011*ΔtrpL* (pSRKGm-rnTrpL, pRK4352) were washed and grown for 4 h in medium without Tc to remove possible effects of Tc on gene expression (Fig. 1E; see also Fig. S2). Then, lacZ'-rnTrpL production was induced with IPTG. After 10 min, Tc was added and the cells were incubated for another 10 min with IPTG and Tc. RNA was isolated at 0, 10 and 20 min (Fig. 1E) and changes in the *rpmA* levels were analyzed. Fig. 1F shows that the *rpmA* level was only decreased if both IPTG and Tc were present in the medium. The *rpmA* level was not changed if lacZ'-rnTrpL production was induced with IPTG in Tc-free medium (t = 10 min in Fig. 1E; see the bar marked with an asterisk in Fig. 1F). Importantly, 10 min after Tc addition to this IPTG-induced culture, the *rpmA* level decreased (t = 20 min in Fig. 1E; see the bar marked with two asterisks in Fig. 1F). Since the *rpmA* decrease was similar at 10 min and 20 min after simultaneous addition of IPTG and Tc (see the two left bars in Fig. 1F), the observed change in the *rpmA* level at 10 min after Tc addition to the IPTG-induced culture (t = 20 min in Fig. 1E) can be attributed to the Tc exposure. This Tc-dependent regulation was specific to *rplUrpmA*, since the level of the *trpC* mRNA was always decreased upon rnTrpL induction, regardless of the presence/absence of Tc (Fig. S3). Together, these results suggested that Tc directly contributes to the down-regulation of *rpmA* by peTrpL and rnTrpL.

The sRNA rnTrpL base pairs with *rplU* and destabilizes *rplUrpmA* mRNA

Next, we tested experimentally the predicted base-pairing between rnTrpL and *rplU* (Fig. 2A). For this, we performed two-plasmid assays in strain 2011*ΔtrpL* using lacZ'-rnTrpL derivatives (transcribed from pSRKTc conferring resistance to Tc) and bicistronic *rplUrpmA'::egfp* reporter constructs (on pSRKGm conferring resistance to Gm; see Fig. S1). Each *rplUrpmA'::egfp* construct was co-induced with wildtype or mutated lacZ'-rnTrpL and fluorescence was measured 20 min after IPTG addition. Fig. 2B shows that L27'-EGFP fluorescence derived from plasmid pSRKGm-rplUrpmA'-egfp was strongly decreased if lacZ'-rnTrpL was co-expressed, in line with the idea that the sRNA binds to *rplU* and thereby induces a reduction of *rplUrpmA'::egfp* mRNA levels. In contrast, sRNA derivatives harboring the GG46,47CC and CG40,41GC mutations, respectively, did not cause this effect. Importantly, compensatory mutations in the *rplUrpmA'::egfp* transcript (CC/GG exchange at positions 221 and 222 of the *rplU* ORF, see Fig. 2A), which were designed to restore the base-pairing to rnTrpL-GG46,47CC, specifically restored the negative effect of the sRNA on fluorescence levels. Similarly, the introduction of a compensatory mutation, G228C, into *rplU* (Fig. 2A) could be shown to cause a down-regulation of the reporter by rnTrpL-CG40,41GC (Fig. 2B). These results validate the base-pairing between rnTrpL

158 and *rplU* and show that even subtle changes in the number of base-pairing interactions may have
159 major consequences for downregulation of *rplUrpmA*.

160 The downregulation of *rplUrpmA* by rnTrpL may be explained by a destabilization of the mRNA.
161 Consistent with this hypothesis, we observed that, upon lacZ'-rnTrpL induction, the half-life of *rpmA*
162 was shortened, while that of the control mRNA *rpoB* was not changed (Fig. 2C). Since the interaction
163 site of the sRNA rnTrpL is located in *rplU*, this result allows us to conclude that the bicistronic
164 *rplUrpmA* mRNA is destabilized by the sRNA.

165

166 **Tc-dependent coimmunoprecipitation with 3xFLAG-peTrpL reveals a new target mRNA and**
167 **antisense RNAs**

168 Based on data shown in Fig. 1, we hypothesized that rnTrpL, peTrpL, Tc and *rplUrpmA* mRNA form a
169 complex in *S. meliloti*. To isolate this complex, we decided to produce an N-terminally triple FLAG-
170 tagged version of TrpL (3×Flag-peTrpL) and to perform coimmunoprecipitation (CoIP) experiments.
171 First, we tested whether 3×Flag-peTrpL is functional. We detected a decrease in the *rpmA* level 10
172 min post IPTG addition to cultures of strain 2011 (pSRKGm-3×Flag-peTrpL, pRK4352) (Fig. 3A).
173 Although this decrease was less pronounced than the decrease caused by wild-type peTrpL, this
174 result suggested that 3×Flag-peTrpL largely retained the functionality of the native peptide.

175 For the CoIP, lysates were prepared at 10 min after IPTG addition to cultures of strain 2011
176 (pSRKGm-3×Flag-peTrpL, pRK4352) and the control strain 2011 (pSRKGm-peTrpL, pRK4352),
177 respectively, both grown in the presence of Gm and Tc. We considered the possibility that the
178 formation of a complex containing peTrpL, rnTrpL and *rplUrpmA* may depend on the presence of Tc.
179 Therefore, after incubation of a lysate with FLAG-tag-antibodies coupled to beads, the beads were
180 divided into two fractions. One half was washed with a Tc-containing buffer (2 µg/ml Tc), while the
181 second half was washed with buffer without Tc. Then, coimmunoprecipitated RNA was purified and
182 analyzed by qRT-PCR. The sRNA rnTrpL was strongly enriched by CoIP with the 3xFLAG-peTrpL, but
183 only if Tc was present in the washing buffer (Fig. 3B). Similarly, *rplUrpmA* could be coprecipitated in a
184 Tc-dependent manner, while none of the control mRNAs (*trpDC, trpE*) could be coprecipitated (Fig.
185 3B). These data support the idea that interactions between the attenuator sRNA rnTrpL, the leader
186 peptide peTrpL and their target mRNA *rplUrpmA* are facilitated by (or even dependent on) the
187 presence of Tc.

188 To identify peTrpL interaction partners, the CoIP-RNA samples were subjected to RNAseq analysis,
189 which revealed an enrichment of RNAs corresponding to three genomic loci (rnTrpL, *rplUrpmA*, and
190 SM2011_c02866) (Fig. 3C). The SM2011_c02866 mRNA encodes the TetR-type transcription
191 regulator SmeR, a repressor of the *smeAB* multidrug efflux pump genes (Eda et al. 2011). The Tc-
192 dependent enrichment of *smeR* was confirmed by qRT-PCR (Fig. 3B).

193 Surprisingly, the RNAseq data also revealed the presence of antisense RNAs (asRNAs)
194 corresponding to *smeR*, *rplUrpmA* and rnTrpL in the CoIP samples (Fig. 3C; see also Fig. S3),
195 possibly indicating an antisense mechanism of gene regulation that involves peTrpL.

196

197 **The peptide peTrpL is involved in the regulation of the multidrug efflux pump operon *smeABR***

198 To test whether peTrpL regulates *smeR*, we analyzed the *smeR* mRNA levels before and after
199 induced production of rnTrpL or peTrpL in a *ΔtrpL* background, in the presence or absence of Tc, as
200 described above for *rplUrpmA* (compare to Fig. 1B). Induction of peTrpL production for 10 min proved
201 to be sufficient for decreasing *smeR* mRNA levels in a Tc-dependent but rnTrpL-independent manner
202 (Fig. 4A). This decrease was (at least in part) due to a destabilization of the *smeR* mRNA (Fig. 4B).
203 Given that *smeR* down-regulation most likely leads to reduced production of the SmeR repressor
204 which, in turn, would result in increased *smeAB* expression, we analyzed the *smeA* mRNA level and
205 found that it was significantly increased at 20 min (but not 10 min) p. i. of peTrpL production (Fig. 4C).
206 This supports the idea that, in the presence of Tc, the rnTrpL-independent destabilization of *smeR*
207 mRNA by peTrpL causes an upregulation of *smeAB*.

208 The *smeR* gene is located downstream of *smeAB* (Eda et al., 2011; Fig. 4F). We found that *smeABR*
209 are cotranscribed upon exposure of strain 2011*ΔtrpL* to Tc (Fig. 4D), a condition under which *smeAB*
210 upregulation, but *smeR* downregulation would be expected. Thus, the posttranscriptional
211 downregulation of *smeR* by peTrpL probably serves to achieve differential expression of *smeAB* and
212 *smeR* despite their cotranscription. According to Fig. 3C, an asRNA is probably involved in this
213 regulation. To test whether a Tc-inducible antisense promoter P_{as} is present downstream of *smeR,* we
214 used plasmid pSUP-PasRegfp harboring a transcriptional fusion of *egfp* to the putative P_{as} (Fig. S1).
215 The level of the reporter mRNA *egfp* was strongly increased after 10 min exposure to Tc or to other
216 known SmeR-effectors: the plant flavonoid genistein (Gs) and the antibiotics chloramphenicol (Cl),
217 erythromycin (Em) and rifampicin (Rf) (Fig. 4E). Kanamycin (Km) and the flavonoid luteolin (Lt), which
218 are not SmeR effectors, were used as negative controls. Thus, transcription of the asRNA As-smeR
219 was induced by the same antimicrobial substances that (also) induce *smeABR* transcription (Eda et
220 al., 2011). Probably, As-smeR is involved in the destabilization of *smeR* mRNA by peTrpL (Fig. 4F).

221

222 **peTrpL increases the multiresistance of *S. meliloti***

223 The data shown in Fig. 4 suggest that peTrpL may contribute to increased resistance towards multiple
224 SmeR effectors. To corroborate this hypothesis, we tested if induction of peTrpL production (using
225 pSRKGm-peTrpL) influences the intrinsic resistance of strain 2011*ΔtrpL* to Tc and natural
226 tetracyclines. As a control, a plasmid was constructed in which the third codon of the ORF was
227 replaced with a stop codon (pSRKGm-peTrpL-3.UAG). Zone of growth inhibition tests revealed an
228 increased resistance (smaller bacterial-free halo) only if the production of peTrpL was induced (Fig. 5A
229 and 5B; Fig. S4). Consistently, induction of ectopic peTrpL production enabled *S. meliloti* to reach
230 higher ODs in liquid cultures containing 0.2 µg/ml Tc, a concentration ten-fold lower than the minimal
231 inhibitory concentration (MIC) (Fig. 5C).

232 Next, we compared strains 2011 and 2011*ΔtrpL*. Both strains reached similar ODs in the absence of
233 Tc, and they failed to grow in medium containing 10 µg/ml Tc, which was half of the concentration

used in our selective media. However, in medium supplemented with 0.2 µg/ml Tc, the parental strain 2011 reached a significantly higher OD compared to the deletion mutant 2011*ΔtrpL* (Fig. 5D), showing that the native *trpL* is important for the Tc resistance of *S. meliloti*.

According to Fig. 4, a Tc-triggered and peTrpL-dependent down-regulation of *smeR* should cause an increased multidrug efflux. To provide additional support for this model, NileRed efflux assays were performed with strain 2011*ΔtrpL* (pSRKGm-peTrpL) and the corresponding EVC in liquid cultures containing 1.5 µg/ml Tc. Fig. 5E shows that the intrinsic efflux pump activity of *S. meliloti* was (only) increased under conditions when peTrpL production was induced.

Finally, we tested whether peTrpL mediates resistance to other SmeR-effectors in addition to Tc. Fig. 5F shows that induced peTrpL production increased the MICs for Cl, Em, Rf and Gs, while, as expected, the MICs for Km and Lt were not affected by peTrpL. In conclusion, peTrpL contributes to the *smeAB*-mediated multiresistance of *S. meliloti*.

Gene regulation in *trans* by two different peTrpL-dependent pathways

The above results suggest that, upon exposure to Tc, the peptide peTrpL contributes to two different regulatory pathways: an rnTrpL-dependent pathway for *rplUrpmA* downregulation and an rnTrpL-independent pathway, in which *smeR* is downregulated. Since the first pathway affects ribosomal genes and Tc inhibits translation, we hypothesized that this pathway is a response to translation inhibition. Thus, we proposed that, in addition to Tc, *rplUrpmA* downregulation should be triggered also by other translation inhibiting antibiotics, such as, Km, Cl and Em, but not by Gs (a tyrosine protein kinase inhibitor) (Akiyama et al., 1987). In contrast, the second rnTrpL-independent pathway should be triggered by the SmeR-effectors Cl, Em and Gs but not by Km, which is not an effector of SmeR.

To test this, strain 2011 was exposed for 10 min to subinhibitory concentrations of the antimicrobial compounds mentioned above, and changes in the levels of *smeR* and *rpmA* were analyzed (Fig. 6A). The results fully supported our hypothesis: i) the *rpmA* level was decreased upon exposure to Km, Cl, Em and Tc, but not Gs, and ii) the *smeR* level was decreased upon exposure to Cl, Em, Gs and Tc, but not Km. Treatment of the deletion mutant 2011*ΔtrpL* revealed no change in the levels of *rpmA* and *smeR* (Fig. S5), supporting the critical role of *trpL* in downregulation of these genes upon exposure to antimicrobial substances. Together, the results shown in Fig. 6A support the existence of two peTrpL-dependent pathways for posttranscriptional regulation.

Based on data shown in Fig. 3B, we proposed that translation-inhibiting antibiotics may be critical for an interaction of peTrpL with rnTrpL and *rplUrpmA*, while SmeR-effectors may be needed for an interaction with *smeR* mRNA. To test this, CoIP with 3×FLAG-peTrpL was conducted 10 min after exposure to Km, Cl or Gs at subinhibitory concentrations. Analysis of the coimmunoprecipitated RNA was in full agreement with our hypothesis (Fig. 6B): i) rnTrpL and *rplUrpmA,* but not *smeR* were enriched in the presence of Km (which causes translation inhibition without being a SmeR-effector), ii) rnTrpL, *rpmA* and *smeR* were enriched in the presence of Cl (which, like Tc, is a translational inhibitor and SmeR-effector; compare to Fig. 3B), and iii) *smeR* (but not rnTrpL and *rplUrpmA)* was enriched in

the presence of Gs (SmeR-effector only). Thus, different antimicrobial compounds seem to promote specific interactions between peTrpL and its RNA targets.

Generation of the sRNA rnTrpL in response to translation inhibition

Is there a functional link between the *trpL* attenuator, translation inhibition and regulation of *rplUrpmA* in *S. meliloti*? Our data, along with earlier studies showing that, in *E. coli*, ribosome pausing in the first half of *trpL* mediates transcription termination between *trpL* and *trpE* (Zurawski et al., 1978), led us to address the question of whether translation inhibition causes rnTrpL generation independently of the Trp availability. We tested whether under conditions of Trp insufficiency (when *trpLE(G)* cotranscription takes place) transcription is terminated downstream of *trpL* upon addition of Tc. We used strain 2011*ΔtrpC,* in which the attenuation can be easily assessed (Bae and Crawford, 1990). Fig. 6C shows that after 4 h of growth under Trp-limiting conditions, rnTrpL was essentially non-detectable in the Northern hybridization. Addition of 1.5 µg/ml Tc to this culture resulted in increased rnTrpL levels, in line with the proposed transcription termination as a consequence of ribosome pausing at the first *trpL* codons. Accordingly, removal of Tc from the medium led again to a decrease in the rnTrpL levels (Fig. 6C).

These results support the idea that bacteria use the uORF *trpL* to sense translation inhibition and respond by releasing an sRNA that down-regulates specific ribosomal genes (Fig. 6D). In addition, these data show that the *trpL* attenuator senses two different signals, Trp availability and translation inhibition.

Conservation of rnTrpL and peTrpL function in other bacteria

Next we tested whether the role of rnTrpL and peTrpL in *rplUrpmA* and *smeR* regulation is conserved in other bacteria. For this we used *Agrobacterium tumefaciens* (which, together with *S. meliloti*, belongs to the *Rhizobiaceae*), and the more distantly related *Bradyrhizobium japonicum* (a *Bradyrhizobiaceae* member). In both species, the mRNA levels of *rpmA* and of their *sme*R homologs were decreased upon overproduction of Atu-rnTrpL and Bja-rnTrpL, respectively (Fig. 7A). Furthermore, the MIC of Tc for *A. tumefaciens* was increased upon overproduction of Atu-peTrpL (Fig. 7B) and overproduction of Bja-peTrpL enabled growth of *B. japonicum* at high Tc concentration (Fig. 7C). Importantly, production of Atu-peTrpL and Bja-peTrpL in *S. meliloti* did not increase resistance in this heterologous host (Fig. S6).

In silico analysis of putative peTrpL peptides from other Rhizobiales revealed several groups of conserved leader peptides that generally conform to the taxonomy (Fig. S7 and Table S1). The consensus peTrpL sequences of the *Sinorhizobium, Agrobacterium* and *Bradyrhizobium* groups are shown in Fig. 7D. A comparison of the sequence logos with the functional data shows that the patterns of evolutionary and sequence conservation are markedly different. The low sequence conservation of peTrpL is in line with its non-functionality in heterologous hosts (Fig. S6).

To determine functionally important aa residues in peTrpL of *S. meliloti*, we performed alanine scanning mutagenesis and tested the functionality of the mutagenized peptides in strain 2011. Compared to the wildtype peTrpL, the strongest effects were caused by Ala substitutions of Thr4, Ser8 and Trp12, respectively. Induced production of these mutated peptides led to an increase in the levels of both *rpmA* and *smeR*, instead of a decrease (Fig. 7E). Surprisingly, Thr4 and Ser8 are not conserved even in the *Sinorhizobium* group (Fig. 7D).

Discussion

In this study, we show that a bacterial uORF, originally known for its role in ribosome-mediated attenuation (Bae and Crawford, 1990), gives rise to a functional regulatory peptide. Our data provide strong evidence that, in *S. meliloti*, the 14-aa leader peptide peTrpL causes a downregulation of *rplUrpmA* expression upon exposure to translation-inhibiting antibiotics, and acts in conjunction with the attenuator sRNA rnTrpL. Moreover, we show that peTrpL has an rnTrpL-independent function in mediating multiresistance. Taken together, these data suggest strikingly multilayered effects of this mRNA leader in *S. meliloti*.

Few other bacterial 5'-UTRs are known to respond to different intercellular signals or to act both in *cis* and in *trans*. The 5'-UTR of *mgtA,* which encodes a Mg^{2+} transporter in *Salmonella,* is one of the few examples of a *cis*-acting attenuator that is capable of sensing disparate signals. It harbors a proline-rich uORF and can respond to proline shortage or a decline in Mg^{2+} concentrations (Park et al., 2010; Chadani et al., 2017). Metabolite-binding riboswitches that can act in *cis* and in *trans* were described in *Listeria* and *Enterococcus* (Loh et al., 2009; DebRoy et al., 2014). The *trpL* attenuator of *S. meliloti* combines similar mechanisms in an exceptional complexity. We show that, in addition to acting as a regulatory RNA both in *cis* and in *trans* (Melior et al., 2019), it senses in *cis* two disparate signals (Trp availability and translation inhibition), and encodes a *trans*-acting peptide. This complexity is further increased because both *trans*-acting products (rnTrpL and peTrpL) regulate more than one gene and are able to act separately and together.

The peptide peTrpL seems to use different mechanisms, since it needs the sRNA rnTrpL only for the destabilization of *rplUrpmA*, but not for *smeR* (a *smeR*-specific sRNA candidate was not coimmunoprecipitated with 3×FLAG-peTrpL). The posttranscriptional regulation by peTrpL seems to be intimately linked to the presence of antibiotics, which obviously promote the interaction with its target mRNAs. Furthermore, the peTrpL function seems to be linked to asRNAs, since *smeR,* *rplUrpmA* and rnTrpL were coimmunoprecipitated with the corresponding asRNAs. While the antibiotic-induced generation of the asRNA As-smeR could explain the *smeR* downregulation without a need for an sRNA (Fig. 4F; Waters and Storz, 2009), the CoIP of RNAs antisense to rnTrpL and *rplUrpmA* is puzzling. According to Fig. 2, the imperfect complementarity between the sRNA rnTrpL and the mRNA *rplUrpmA* is necessary for the peTrpL-dependent mRNA destabilization, and such complementarity is usually needed for a conventional regulation by base-pairing sRNAs in bacteria, without a need for asRNAs (Waters and Storz, 2009).

The attenuator sRNA rnTrpL also seems to use different mechanisms because, in contrast to *rplUrpmA*, the destabilization of its target mRNAs *sinI* (Baumgardt et al., 2016) and *trpDC* (Melior et al., submitted) does not depend on peTrpL or exposure to antibiotics. The need for peTrpL and an antibiotic for *rplUrpmA* downregulation may serve to redirect rnTrpL from other mRNAs (*trpDC*, *sinI*) to this target of interest under the conditions of translation inhibition. The antibiotic-triggered downregulation of *rplUrpmA* probably represents a novel posttranscriptional mechanism that may be used to adjust the production and/or function(s) of the protein biosynthesis machinery. Lower levels of *rplUrpmA* mRNA may negatively influence ribosome biogenesis and/or result in ribosomes lacking the L21 and L27 proteins. While the function of L21 is not clear, *E. coli* L27-deficient mutants were shown to have reduced peptidyl transferase activities (Maguire et al., 2005). Interestingly, it was shown previously that a two-fold reduction of *rplUrpmA* expression in *Pseudomonas aeruginosa* leads to an increased expression of multidrug efflux pump genes and increased resistance to aminoglycosides. This was explained by attenuation of transcription termination, caused by pausing of L21- and L27-less ribosomes (Lau et al., 2012). It therefore seems reasonable to suggest that, in *S. meliloti*, the down-regulation of *rplUrpmA* by rnTrpL and peTrpL may have similar adaptation effects mediated by specific changes in translation.

The observed generation of the sRNA rnTrpL upon translation inhibition, even under conditions of Trp insufficiency (Fig. 6C and 6D), shows how bacteria can make use of a uORF and mutually exclusive RNA structures of a well-known attenuator for alternative purposes. The rnTrpL sRNA production upon ribosome pausing in the 5'-part of the uORF *trpL* may have additional implications. We note that, in all *Sinorhizobium* species, two Asn and one Gln codon(s) are located in the first half of *trpL*. Pausing of the ribosome at these codons, for example upon shortage of aminoacylated tRNA-Asn and tRNA-Gln, could also result in rnTrpL production. Thus, *trpL* is well-suited for the sensing of nitrogen depletion in *Sinorhizobium*. In most ribosome-dependent transcription attenuators of aa biosynthesis operons, the relevant aa codons are located in the 3'-half of the uORF (Vitreschak et al., 2004). Translation inhibition at such attenuators would also generate sRNAs with potential functions in *trans*.

Unexpectedly, our CoIP analyses revealed a function of peTrpL in the posttranscriptional regulation of the multidrug efflux pump operon *smeABR*. SmeR is a homolog of the multidrug-binding repressor TtgR from *Pseudomonas putida* (Teran et al., 2006), which explains its interactions with several effectors, while the co-transcription of the *smeR* repressor gene together with the *smeAB* efflux pump genes explains the need for differential regulation at the posttrancriptional level. The observed peTrpL-dependent down-regulation of *smeR* followed by upregulation of *smeA* (Fig. 5), the increase in the cellular efflux activity, and the MIC increase observed for all tested SmeR-effectors (Fig. 6), clearly show the key role of peTrpL in multiresistance. Importantly, this function and even the function of peTrpL in *rplUrpmA* downregulation is conserved among Alphaproteobacteria, despite the low conservation of its sequence (Fig. 7). This high sequence divergence might be forced by the (at least) dual function in *trans* of the leader peptide. It probably reflects molecular adaptation to (co-evolution with) interaction partners in the respective host.

The peTrpL-mediated resistance of *S. meliloti* and other Alphaproteobacteria, including the plant pathogen *A. tumefaciens*, is probably crucial for survival in soil, the rhizosphere, and plants, where

exposure to antimicrobial compounds is common. Indeed, the SmeAB efflux pump is known to be important for nodulation competitiveness (Eda et al., 2011). Bacterial strategies that ensure survival at high antibiotic concentrations and increase the competitiveness at subinhibitory concentrations are relevant from both an evolutionary and medical point of view (D'Costa et al., 2011; Nelson and Levy, 2011; Anderson and Hughes, 2014). Although *S. meliloti* is a soil bacterium with no medical relevance, it is a major model organism for studying interactions between bacteria and higher organisms (Jones et al., 2007). The identification of an attenuator leader peptide as a conserved player in the intrinsic bacterial resistance to antibiotics is interesting for two reasons: first, this new knowledge opens new perspectives in understanding the bacterial physiology and evolution, and second, it potentially provides new targets for antibacterial control.

In summary, our work shows the role of the peptide peTrpL in two different posttranscriptional pathways (triggered by translation inhibitors or SmeR effectors, respectively) in *trans*, broadens the target spectrum of the attenuator sRNA rnTrpL, and demonstrates the exceptionally complex regulatory functions exerted by the *trpL*-containing mRNA leader. The data obtained in this study encourage future detailed analyses of novel physiological roles of bacterial attenuator RNAs and the leader peptides encoded by these RNAs.

Material and Methods

Cultivation of bacteria and conjugation

E. coli strains were cultivated in LB supplemented with appropriate antibiotics: Tetracycline (Tc, 20 µl/ml), gentamycin (Gm, 10 µg/ml), ampicillin (200 µg/ml). TY was used as growth medium for prototrophic *S. meliloti* and *A. tumefaciens* strains (Baumgardt et al., 2016). Auxotrophic *S. meliloti* 2011*ΔtrpC* strains were grown in minimal GMX medium (Schlüter et al., 2010) supplemented with L-tryptophan (Trp) as indicated in Fig. 6. *B. japonicum* was grown in PSY medium as described (Hahn et al., 2017). Liquid cultures of Alphaproteobacteria were cultivated semiaerobically (30 ml medium in a 50 ml Erlenmayer flask with shaking at 140 r. p. m.) at 30°C to an OD_{600nm} of 0.5, and then processed further. Antibiotics in selective plates or liquid media for Alphaproteobacteria were used at the following concentrations, unless stated otherwise: Tetracycline (20 µg/ml for *S. meliloti* and *A. tumefaciens*; *B. japonicum* was cultivated with 25 µg/ml Tc in liquid and 50 µg/ml Tc on plates), gentamycin (10 µg/ml in liquid cultures and 20 µg/ml in plates), streptomycin (250 µg/ml), spectinomycin (100 µg/ml). IPTG was added to a final concentration of 1 mM. For growth experiments in 96-well microtiter plates, 300 µl culture (diluted to an OD_{600nm} of 0.1) per well was used. Plates were incubated on the shaker (140 r. p. m.) at 30 °C for 60 h (till the cultures entered the stationary phase).

Constructed plasmids were transferred to *S. meliloti*, *A. tumefaciens* or *B. japonicum* by diparental conjugation with *E. coli* S17-1 as the donor. Bacteria were mixed, washed in saline and spotted onto a sterile membrane filter, which was placed onto a TY plate without antibiotics. After incubation for at least 4 h (for *S. meliloti* and *A. tumefaciens*) or 3 days (for *B. japonicum*) at 30 °C, serial dilutions were spreaded on agar plates with selective antibiotics.

425 **Cloning procedures and plasmid characteristics**

426 Plasmid preparation, restriction analysis, purification of DNA fragments from agarose gels, and cloning
427 procedures were performed as described by Sambrook et al. (1989). FastDigest restriction enzymes
428 and Phusion polymerase were used routinely for cloning in *E. coli*. PCR amplicons were first cloned in
429 pJet1.2/blunt and the inserts were then subcloned into the conjugative, broad-host range vectors
430 pRK4352, pSRKGm, pSRKTc (which can replicate in *S. meliloti* and *A. tumefaciens*) or in pRJ-MCS
431 (used for chromosomal integration in *B. japonicum*). Alternatively, for very short inserts (e.g. *trpL*
432 ORFs with codons exchanged for synonymous codons, or with mutated codons), complementary
433 oligonucleotides were annealed and the resulting double-strand DNA with suitable single-stranded,
434 cohesive ends, was cloned directly into the desired conjugative plasmids. Insert-containing plasmids
435 were analyzed by Sanger sequencing with plasmid-specific primers (sequencing service by Microsynth
436 Seqlab, Göttingen, Germany) prior to conjugation. All oligonucleotides (primers) are listed in Table S3.
437 They were synthesized by Microsynth, Balgach (Switzerland).

438 All plasmids are listed in Table S2. pRK-rnTrpL is a pRK4352 derivative. It leads to constitutive
439 transcription of rnTrpL in *S. meliloti*. Plasmids pRK-rnTrpL-AU1,2UA, pRK-rnTrpL-CG40,41GC, pRK-
440 rnTrpL-G44C and pRK-rnTrpL-GG46,47CC are pRK-rnTrpL derivatives harboring the indicated
441 mutations in the rnTrpL sequence. In the rnTrpL-AU1,2UA, the start codon was exchanged for a stop
442 codon, thus inactivating the *trpL* sORF. The CG40,41GC mutation causes an Arg/Ala exchange in
443 peTrpL and weaker base-pairing with *rplU*, the mutations G44C weakens the base pairing with *rplU*
444 and changes the *trpL* stop codon to a sense codon, and the mutation GG46,47CC, which is located
445 downstream of the *trpL* stop codon, weakens the base-pairing with *rplU.*

446 Plasmids pSRKTc-rnTrpL and pSRKGm-rnTrpL allow for IPTG-inducible transcription of the
447 recombinant rnTrpL derivative lacZ'-rnTrpL (Melior et al., submitted). In contrast to the leaderless wild
448 type (wt) rnTrpL, which starts directly with the ATG of *trpL* (Bae and Crawford, 1990), the rnTrpL
449 variant harbors the *lacZ* 5'-UTR with a ribosome binding site. Its capability to act in *trans* and to
450 downregulate *trpDC* was shown previously (Melior et al., submitted). Plasmid pSRKGm-peTrpL allows
451 for IPTG inducible production of peTrpL It contains the sORF *trpL* with several synonymous nucleotide
452 substitutions (to avoid RNA-based effects), but without rare codons (to avoid toxicity; Zahn, 1996).
453 Plasmid pSRKGm-3xFLAG-peTrpL harbors N-terminally fused codons for a triple FLAG-tag.

454 To construct pSRKGm-rplUrpmA'-egfp, primers NdeI-rplU-fw and 5'-egfp-rpmA-re were used to
455 amplify the *rplUrpmA'* part of the construct, while *egfp* was amplified with primers rpmA-egfp-fw and
456 XbaI-egfp-re. For overlapping PCR, primers NdeI-rplU-fw and XbaI-egfp-re were used, and the PCR
457 product encompassing *rplUrpmA'::egfp* was cloned into pJet1.2/blunt and then subcloned into
458 pSRKGm. IPTG-induced transcription of the bicistronic *rplUrpmA'::egfp* mRNA from pSRKGm-
459 rplUrpmA'-egfp allows for production of L21 and the fusion protein L27'-EGFP, which contains only the
460 first three N-terminal aa of L27 fused to the third aa of EGFP (Fig. S1). To introduce compensatory
461 mutations into the *rplUrpmA'::egfp* reporter, site-directed mutagenesis of pJet-rplUrpmA'-egfp was
462 performed. Primer pair rplU-G-228-C-FW and rplU-G-228-C-RV was used for one nucleotide
463 exchange, thus re-establishing the base pairing or *rplU* to the nucleotide at position 40 in rnTrpL (re-
464 establishing the influence of rnTrpL-CG40,41GC on *rplUrpmA*; see Fig. 2A). Further, primer pair rplU-

CC-222-GG-FW and rplU-CC-222-GG-RV was used for compensatory mutations re-establishing the base pairing with rnTrpL-GG46,47CC. The mutated inserts were then subcloned to create pSRKGm-rplU-CC221,222GG-rpmA'-egfp and pSRKGm-rplU-G228C-rpmA'-egfp.

To construct pSUP-PasRegfp, approximately 200 bp upstream of the putative transcription start site (TSS) of the antisense RNA As-smeR (according to the RNAseq data, see also Fig. 3C and Fig. 4F) was amplified using primers EcoRI-asP-smeR-f and asP-smeR-sSD-rev. The first two nucleotides downstream of the putative TSS were included in the reverse primer, which in addition contained the sequence of a typical bacterial ribosome binding site and the 5'-sequence of *gfp*. The *gfp* sequence of plasmid pLK64 was amplified with primers sSD-egfp-f and PstI-egfp-rev, and the two PCR products were used for overlapping PCR with primers EcoRI-asP-smeR-f and PstI-egfp-rev. The resulting PCR product was cloned into plasmid pSUP202pol4-exoP, which contains 300 nt of the 3' exoP region as a suitable chromosomal integration site, and was cut with EcoRI and PstI (Schlüter et al., 2015). The resulting plasmid pSUP-PasRegfp was used to analyze the antibiotic-induced transcription from a putative antisense promoter located downstream of *smeR*, using the *egfp* mRNA as reporter. Since pSUP-PasRegfp confers Tc resistance, it was necessary to incubate *S. meliloti* strains with chromosomally integrated pSUP-PasRegfp overnight without Tc (essentially all cells retained the plasmid, as revealed by qPCR analysis), before adding Tc again to test for induced promoter activity by qRT-PCR analysis of the reporter *egfp* mRNA.

Zone of growth inhibition tests

For the zone of growth inhibition tests, strains 2011*ΔtrpL* (pSRKGm-peTrpL) and 2011*ΔtrpL* (pSRKGm-peTrpL-3.UAG) were used. 15 ml bottom TY agar was overlayed with 10 ml TY top agar mixed with 1 ml *S. meliloti* culture (OD_{600nm} of 0.5). The bottom and the top agar were supplemented with 20 µg/ml Gm. After solidification of the top agar, a Whatman paper disk was placed in the middle of the plate and 5 µl Tc solution (10 µg/µl in 70% ethanol) were applied onto the disk. Plates were incubated over night at 30 °C, before measuring the diameter of the zone of growth inhibition.

EGFP fluorescence measurement

S. meliloti 2011*ΔtrpL* strains containing two plasmids (pSRKGm- and pSRKTc- constructs for IPTG-induced expression of *egfp* reporter fusions and the sRNA, respectively), were cultivated in TY with Gm and Tc to an OD_{600nm} of 0.5 and then the production of an EGFP fusion protein and the regulatory sRNA was induced simultaneously with 1 mM IPTG for 20 min. Then 300 µl of the cultures were transferred to a 96-well microtiter plate and EGFP fluorescence was measured on a Tecan Infinite M200 reader. ODs were also measured on the Tecan reader and used for normalization.

NileRed efflux assay

The efflux assay was performed essentially as described by Bohnert et al. (2010). 10 ml of a *S. meliloti* culture was harvested. The pellet was washed in 20 mM potassium phosphate buffer (pH 7.0) (PPB) containing 1 mM $MgCl_2$, and resuspended in PPB adjusting the OD_{600nm} to 1.0. The cell suspension was incubated for 15 min at room temperature. 2 ml aliquots were transferred into glass tubes and the efflux pump inhibitor carbonyl cyanide 3-chlorophenylhydrazone (CCCP) was added at a final

concentration of 25 mM (5 mM stock solution in 50% DMSO). After 15 min 5 mM NileRed dye was added (a stock solution of 5 mM in 10% dimethyl formamide, 90% ethanol) and the cell suspension was incubated on a shaker (140 r. p. m.; 30 °C) for 3 h, followed by a 60 min incubation without shaking at room temperature and centrifugation for 5 min at 4,400 r. p. m. in the tabletop centrifuge. Supernatant was entirely removed and cells were resuspended in 1 ml PPB. Immediately thereafter 0.3 ml of this cell suspension was transferred to a 96 well microtiter plate and 15 µl of 1 M glucose was added to trigger NileRed efflux. Fluoresence of the cell suspension was followed over 1500 sec (excitation at 552 n., and emission at 636 nm) on the Tecan reader.

RNA purification

To purify total RNA of *S. melililoti* and *A. tumefaciens* for Northern blot hybridization and qRT-PCR analysis, 15 ml culture (OD_{600} = 0.5) was filled into tubes with ice rocks (corresponding to a volume of 15 ml) and pelleted by centrifugation at 6,000 g for 10 min at 4 °C. The pellet was resuspended in 250 ml TRIzol. Cells were lysed in a shacking mill (4 °C) with glass beads, two times for 15 min, interrupted by incubation at 65 °C for 10 min. After addition of 750 µl TRIzol to the samples, RNA was isolated according to the manufacturer instructions. To remove residual RNases, the isolated RNA was additionally purified with hot-phenol, phenol:chloroform:isoamylalcohol and chloroform:isoamylalcohol, and then ethanol-precipitated. For RNA half-live measurements, 1 ml bacterial culture was added to 2 ml RNAprotect Bacteria Reagent (Qiagen) and RNA was isolated using RNeasy columns (Qiagen). RNA from *B. japonicum* was isolated with hot phenol. The washed and dried RNA was resuspended in 30 µl of ultrapure water. RNA concentration and purity was analyzed by measuring absorbance at 260 nm and 280 nm. 10% polyacrylamide-urea gels and staining with ethidium bromide were used to control the integrity of the isolated RNA. For qRT-PCR RNA, 10 µg samples were digested with 1 µl TURBO-DNase for 30 minutes to remove remaining DNA. PCR with *rpoB*-specific primers was performed for each sample, to check for residual DNA. The DNA-free RNA was then diluted to a concentration of 20 ng/µl for the qRT-PCR analysis.

Northern Blot hybridization

Total RNA (10 µg) was denatured in urea-formamide containing loading buffer at 65 °C, placed on ice and loaded on 1 mm thick, 20 x 20 cm, 10% polyacrylamide-urea gel. Separation by electrophoresis in TBE buffer was performed at 300 V for 4 h. Then the RNA was transferred to a positively charged nylon membrane for 2 h at 100 mA using a Semi-Dry Blotter. After crosslinking of the RNA to the membrane by UV light, the membrane was pre-hybridized for 2 h at 56 °C with a buffer containing 6× SSC, 2.5× Denhardts solution, 1% SDS and 10 µg/ml Salmon Sperm DNA. Hybridization was performed with radioactively labeled oligonucleotides (see Table S3) in a solution containing 6× SSC, 1% SDS, 10 µg/ml Salmon Sperm DNA for at least 6 h at 56 °C. The membranes were washed twice for 2 to 5 min in 0.01% SDS, 5× SSC at room temperature. Signal detection was performed with a BioRad molecular imager and the Quantity One (BioRad) software. For quantification, the intensity of the sRNA bands was normalized to the intensity of the 5S rRNA. For re-hybridization, membranes were stripped for 20 min at 96 °C in 0.1% SDS.

Radioactive labeling of oligonucleotide probes

5`-labeling of 10 pmol oligonucleotide was performed with 5 U T4 polynucleotide kinase (PNK) and 15 µCi [γ-^{32}P]-ATP in a 10 µl reaction mixture containing buffer A provided by the manufacturer. The reaction mixture was incubated for 60 min at 37 °C. After adding 30 µl water, unincorporated nucleotides were removed using MicroSpin G-25 columns.

Reverse transcription PCR (RT-PCR) und real time, quantitative RT-PCR (qRT-PCR)

For RT-PCR, first cDNA synthesis was performed with DNA-free RNA using the reverse primer. Then, PCR using both the forward and the reverse primers, was conducted. For analysis of relative steady state levels of specific RNAs by real time RT-PCR (qRT-PCR), the Brilliant III Ultra Fast SYBR® Green QRT-PCR Mastermix (Agilent) was used. Each 10 µl reaction mixture contained 5 µl Master Mix (supplied), 0.1 µl DTT (100 mM; supplied), 0.5 µl Ribo-Block solution (supplied), 0.4 µl water, 1 µl of each primer (10 pmol/µl), and 2 µl RNA (20 ng/µl). Routinely, first only the primer needed for cDNA synthesis was added to the reaction mixture. After cDNA synthesis and incubation for 10 min at 96 °C to inactivate the reverse transcriptase, the probes were cooled to 4 °C, the second primer was added, and PCR was performed starting with 5 min incubation at 96 °C. For one-step qRT-PCR (Fig. 3B), both primers were added simultaneously, before the cDNA synthesis step. Used primer pairs and their efficiencies (as determined by PCR using serial two-fold dilutions of RNA) are listed in Table S3. The qRT-PCR reaction was performed in a spectrofluorometric thermal cycler (Biorad). The quantification cycle (Cq), was set to a cycle at which the curvature of the amplification is maximal (Bustin et al., 2009). As a reference gene for determination of steady-state mRNA levels, *rpoB* (encodes the β subunit of RNA polymerase) was used (Baumgardt et al., 2016). For half-life determination, it was necessary to use the stable 16S rRNA as a reference molecule. To achieve similar Cq of mRNA and 16S rRNA, 2 µl RNA with a concentration of 0.002 ng/µl was used in a 10 µl reaction for real-time RT-PCR with 16S rRNA specific primers. Cq-values of genes of interest and the reference gene were used in the Pfaffl-formula to calculate fold changes of mRNA amounts (Pfaffl, 2001).

For qRT-PCR analysis of total RNA, the real-time PCR of the gene of interest (e.g. *rpmA*) and of the reference gene *rpoB* were performed using portions of the same DNA-free RNA sample. For qRT-PCR analysis of CoIP-RNA, the real-time RT-PCR of the gene of interest was performed using a CoIP-RNA sample, while total RNA of the same culture (harvested prior cell lysis for CoIP) was used for the *rpoB* real time RT-PCR.

qPCR

To determine plasmid-DNA levels, qPCR with plasmid-specific primers (Table S3) and Power SYBR® PCR Mastermix were performed. The provided PCR master mix included all components necessary for performing real-time PCR except primers, template, and water, which were added as described for qRT-PCR. The qPCR reaction and quantification were performed like described for qRT-PCR analysis of total RNA.

Coimmunoprecipitation of RNA with 3xFLAG-peTrpL

The strains containing the triple FLAG-tagged leader peptide *S. meliloti* 2011 (pSRKGm-3xFLAG-peTrpL, pRK4352), as well as the control *S. meliloti* 2011 (pSRKGm-peTrpL, pRK4352), were grown

in 1 l TY with Gm and Tc, before inducing them with 1 mM IPTG for 10 minutes at OD_{600} of 0.5. Cell pellet was resuspended in 5 ml lysis buffer containing 20 mM Tris, pH of 7.5, 150 mM KCl, 1 mM $MgCl_2$, 1 mM DTT, lysozyme, 2 µg/ml Tc and 1 pill protease inhibitor per 40 ml buffer. Cells were lysed by sonication and 40 µl anti-FLAG antibody-bound magnetic beads were added to the cleared lysate. After incubation at 4 °C for 2 h, the beads were collected and split into two portions. One sample was washed 3 times with 500 µl lysis buffer containing 2 µg/ml Tc, while the second sample was washed without tetracycline in the buffer. Purification of CoIP RNA was performed using TRIzol, without subsequent hot-phenol treatment.

Computational analysis

281 genomes of Rhizobiales were downloaded from GenBank (Benson et al., 2013) at August 2018. Intergenic regions of length 300 upstream of the gene *trpE* were extracted. We then considered all open reading frames containing at least two consecutive UGG codons and converted them into amino acid sequences of candidate leader peptides. The peptides were aligned using MUSCLE with default parameters (local alignment, open gap penalty –10, extend gap penalty –1) (Edgar, 2004). Hanging N-termini were trimmed manually, retaining the condition that candidate leader peptides should start with methionine. Phylogenetic trees were constructed based on the constructed distance matrix using R package “cluster” with default parameters (Maechler et al., 2018) by the Ward2 method (Murtagh and Legendre, 2014) and visualized using R package “ggplot2” (Wickham, 2016). Sequence logos were constructed using WebLogo (Crooks et al., 2004). The validity of predicted leader peptides was assessed by construction of alternative RNA secondary structures characteristic of attenuators using ad hoc Python scripts for the identification of overlapping RNA helices.

Data availability

The RNA-Seq and RIP-Seq data discussed in this publication have been deposited in NCBI's Gene Expression Omnibus (Edgar *et al*., 2002); accession number GSE118689.

Acknowledgments

We thank Marta Robledo for helpful discussions and Janina Gerber for help in some experiments. The peTrpL computational analysis was initiated at the Summer School of Molecular and Theoretical Biology supported by the Zimin Foundation.

Author contributions

Conceptualization, E.EH., H.M.; Methodology, E.E.H., H.M., S.M., Z.C.; Investigation, H.M., S.L., M.S., S.M., R.S., S.A., S.B.W., A.S., K.B.; Formal analysis, H.M., S.L., M.S., K.U., S.M., A.S., Z.C., C.H.A.; Writing – Original Draft, E.E.H., H.M., J.Z.; Writing – Review and Editing, E.E.H., H.M., S.M., Z.C., J.Z., C.H.A.; Visualization, E.E.H., H.M., M.S., S.L.; Supervision, E.E.H., Z.C.; Funding Acquisition, E.E.H.

Funding

This work was funded by DFG (EV42/6-1, Ev42/7-1 in SPP2002, GRK2355). S.L. was supported by the China Scholarship Council (No. 201708080082); Z.C. was supported by the Russian Science Foundation (18-14-00358).

Declaration of interests

The authors declare no competing interests.

References

Akiyama, T., Ishida, J., Nakagawa, S., Ogawara, H., Watanabe, S., Itoh, N., Shibuya, M., and Fukami, Y. (1987) Genistein, a specific inhibitor of tyrosine-specific protein kinases. J. Biol. Chem. 262, 5592-5595.

Andersson, D.I., and Hughes, D. (2014) Microbiological effects of sublethal levels of antibiotics. Nat. Rev. Microbiol. 12, 465-478.

Andrews, S.J., and Rothnagel, J.A. (2014) Emerging evidence for functional peptides encoded by short open reading frames. Nat. Rev. Genet. 15,193-204.

Bae,Y.M. and Crawford, I.P. (1990) The *Rhizobium meliloti trpE(G)* gene is regulated by attenuation, and its product, anthranilate synthase, is regulated by feedback inhibition. J. Bacteriol. 172, 3318-3327.

Baumgardt, K., Šmídová, K., Rahn, H., Lochnit, G., Robledo, M. and Evguenieva-Hackenberg, E. (2016) The stress-related, rhizobial small RNA RcsR1 destabilizes the autoinducer synthase encoding mRNA *sinI* in *Sinorhizobium meliloti*. RNA Biol., 13, 486-499.

Benson, D.A., Cavanaugh, M., Clark, K., Karsch-Mizrachi, I., Lipman, D.J., Ostell, J., and Sayers, E.W. (2013) GenBank. Nucleic Acids Res. 41, D36-42.

Bohnert, J. A., Karamian, B., and Nikaido, H. (2010) Optimized Nile Red Efflux Assay of AcrAB-TolC Multidrug Efflux System Shows Competition between substrates. Antimicrob. Agents. Chemother. 54, 37770-3775.

Bustin, S. A., Benes, V., Garson, J. A., Hellemans, J., Huggett, J., Kubista, M., Mueller, R., Nolan, T., Pfaffl, M. W., Shipley, G. L., et al. (2009) The MIQE guidelines: minimum information for publication of quantitative real-time PCR experiments. Clin. Chem. 55, 611-622.

Cabrera-Quio, L.E., Herberg, S., and Pauli, A. (2016) Decoding sORF translation - from small proteins to gene regulation. RNA Biol. 13, 1051-1059.

Casse, F., Boucher, C., Julliot, J.S., Michel, M. and Denarie, J. (1979) Identification and characterization of large plasmids in *Rhizobium meliloti* using agarose-gel electrophoresis. *Gen Microbiol.* 113, 229-242.

Chadani, Y., Niwa, T., Izumi, T., Sugata, N., Nagao, A., Suzuki, T., Chiba, S., Ito, K., and Taguchi, H. (2017) Intrinsic Ribosome Destabilization Underlies Translation and Provides an Organism with a Strategy of Environmental Sensing. Mol. Cell 68, 528-539.e5.

650 Crooks, G.E., Hon, G., Chandonia, J.M., and Brenner, S.E. (2004) WebLogo: A sequence logo
651 generator, Genome Research, 14, 1188-1190

652 Dar, D., Shamir, M., Mellin, J.R., Koutero, M., Stern-Ginossar, N., Cossart, P., and Sorek, R. (2016)
653 Term-seq reveals abundant ribo-regulation of antibiotics resistance in bacteria. Science
654 352(6282):aad9822.

655 Dar, D., and Sorek, R. (2017) Regulation of antibiotic-resistance by non-coding RNAs in bacteria.
656 Curr. Opin. Microbiol. 36, 111-117.

657 D'Costa, V.M., King, C.E., Kalan, L., Morar, M., Sung, W.W., Schwarz, C., Froese, D., Zazula, G.,
658 Calmels, F., Debruyne, R., et al. (2011) Antibiotic resistance is ancient. Nature. 477, 457-461.

659 DebRoy S, Gebbie M, Ramesh A, Goodson JR, Cruz MR, van Hoof A, Winkler WC, and Garsin DA.
660 (2014) Riboswitches. A riboswitch-containing sRNA controls gene expression by sequestration of a
661 response regulator. Science 345, 937-940.

662 Eda, S., Mitsui, H., and Minamisawa, K. (2011) Involvement of the *smeAB* multidrug efflux pump in
663 resistance to plant antimicrobials and contribution to nodulation competitiveness in *Sinorhizobium*
664 *meliloti*. Appl. Environ. Microbiol. 77, 2855-2862.

665 Edgar, RC. (2004) MUSCLE: multiple sequence alignment with high accuracy and high throughput.
666 Nucleic Acids Res. 32, 1792-1797.

667 Edgar, R., Domrachev, M., and Lash, A.E. (2002) Gene Expression Omnibus: NCBI gene expression
668 and hybridization array data repository. Nucleic Acids Res. 30, 207-210.

669 Fischer HM, Babst M, Kaspar T, Acuna G, Arigoni F, Hennecke H.(1993) One member of a gro-ESL-
670 like chaperonin multigene family in *Bradyrhizobium japonicum* is co-regulated with symbiotic nitrogen
671 fixation genes. EMBO J. 12, 2901-2912.

672 Gaballa, A., Antelmann, H., Aguilar, C., Khakh, S., Song, K.B., Smaldone, G.T., and Helmann, J.D.
673 (2008) The *Bacillus subtilis* iron-sparing response is mediated by a Fur-regulated small RNA and three
674 small, basic proteins. Proc. Natl. Acad. Sci. U. S. A. 105, 11927-11932.

675 Jones, K.M., Kobayash,i H., Davies, B.W., Taga, M.E., and Walker, G.C. (2007) How rhizobial
676 symbionts invade plants: the Sinorhizobium-Medicago model. Nat. Rev. Microbiol. 5, 619-633.

677 Hahn, J., Thalmann, S., Migur, A, von Boeselager, R.F., Kubatova, N., Kubareva, E., Schwalbe, H.,
678 and Evguenieva-Hackenberg, E. (2017) Conserved small mRNA with an unique, extended Shine-
679 Dalgarno sequence. RNA Biol. 14, 1353-1363.

680 Kereszt, A., Mergaert, P., Montiel, J., Endre, G., and Kondorosi, É. (2018) Impact of Plant Peptides on
681 Symbiotic Nodule Development and Functioning. Front. Plant Sci. 9,1026.

682 Khan, S.R., Gaines, J., Roop, R.M. 2nd, and Farrand, S.K. (2008) Broad-host-range expression vectors
683 with tightly regulated promoters and their use to examine the influence of TraR and TraM expression
684 on Ti plasmid quorum sensing. Appl. Environ. Microbiol. 74, 5053-5062.

685 Kondo, T., Hashimoto, Y, Kato, K., Inagaki, S., Hayashi, S., and Kageyama, Y. (2007) Small peptide
686 regulators of actin-based cell morphogenesis encoded by a polycistronic mRNA. Nat. Cell. Biol. 9,
687 660–665.

688 Lau, C.H., Fraud, S., Jones, M., Peterson, S.N., and Poole, K. (2012) Reduced expression of the *rplU-*
689 *rpmA* ribosomal protein operon in *mexXY*-expressing pan-aminoglycoside-resistant mutants of
690 *Pseudomonas aeruginosa*. Antimicrob. Agents. Chemother. 56, 5171-5179.

691 Loh, E., Dussurget, O., Gripenland, J., Vaitkevicius, K., Tiensuu, T., Mandin, P., Repoila, F.,
692 Buchrieser, C., Cossart, P., Johansson, J. (2009) A *trans*-acting riboswitch controls expression of the
693 virulence regulator PrfA in *Listeria monocytogenes*. Cell 139,770-779.

694 Lovett, P.S., and Rogers, E.J. (1996) Ribosome regulation by the nascent peptide. Microbiol Rev. 60,
695 366-385.

696 Maguire, B.A., Beniaminov, A.D, Ramu, H., Mankin, A.S., and Zimmermann R.A. (2005) A protein
697 component at the heart of an RNA machine: the importance of protein l27 for the function of the
698 bacterial ribosome. Mol. Cell. 20, 427-435.

699 Mank, N.N., Berghoff, B.A., Hermanns, Y.N., and Klug, G. (2012) Regulation of bacterial
700 photosynthesis genes by the small noncoding RNA PcrZ. Proc. Natl. Acad. Sci. U. S. A. 109, 16306-
701 11631.

702 Maechler, M., Rousseeuw, P., Struyf, A., Hubert, M., Hornik, K. (2018). cluster: Cluster Analysis
703 Basics and Extensions. R package version 2.0.7-1.

704 McIntosh, M., Krol, E., and Becker, A. (2008) Competitive and Cooperative Effects in Quorum-
705 Sensing-Regulated Galactoglucan Biosynthesis in *Sinorhizobium meliloti*. J. Bacteriol. 190, 5308-
706 5317.

707 Melior, H., Li, S., Madhugiri, R., Stötzel, M., Azarderakhsh, S., Barth-Weber, S., Baumgardt, K.,
708 Ziebuhr, J., Evguenieva-Hackenberg, E. (2019) Transcription attenuation-derived small RNA rnTrpL
709 regulates tryptophan biosynthesis gene expression in *trans*. Nucleic Acids Res., in press.

710 Merino,E., Jensen,R.A., and Yanofsky,C. (2008) Evolution of bacterial *trp* operons and their regulation.
711 Curr. Opin. Microbiol., 11, 78-86.

712 Murtagh, F., and Legendre, P. (2014) Ward's hierarchical agglomerative clustering method: which
713 algorithms implement Ward's criterion? Journal of Classification, 31, 274-295.

714 Nelson, M.L., and Levy, S.B. (2011) The history of the tetracyclines. Ann. N. Y. Acad. Sci. (2011)
715 1241, 17-32.

716 Omasits, U., Varadarajan, A.R., Schmid, M., Goetze, S., Melidis, D., Bourqui, M., Nikolayeva, O.,
717 Québatte, M., Patrignani, A., Dehio, C., et al. (2017) An integrative strategy to identify the entire
718 protein coding potential of prokaryotic genomes by proteogenomics. Genome Res. 27, 2083-2095.

719 Park, S.Y., Cromie, M.J., Lee, E.J., and Groisman, E.A. (2010) A bacterial mRNA leader that employs
720 different mechanisms to sense disparate intracellular signals. Cell 142,737-748.

721 Park, H., McGibbon, L.C., Potts, A.H., Yakhnin, H., Romeo, T., and Babitzke, P. (2017) Translational
722 Repression of the RpoS Antiadapter IraD by CsrA Is Mediated via Translational Coupling to a Short
723 Upstream Open Reading Frame. MBio. 8. pii: e01355-17.

724 Pfaffl, M.W. (2001) A new mathematical model for relative quantification in real-time RT-PCR. *Nucleic*
725 *Acids Res.* 29, e45.

726 Regensburger, B. and Hennecke, H. (1983) RNA polymerase from *Rhizobium japonicum*. Arch.
727 Microbiol., 135, 103-109.

728 Sambrook, J., Fritsch, E.F., Maniatis, T. (1989) Molecular cloning: A laboratory manual. 2. Cold Spring
729 Harbor Laboratory Press, Cold Spring Harbor, NY.

730 Schäfer, A., Tauch, A., Jäger, W., Kalinowski, J., Thierbach, G., and Pühler, A. (1994) Small
731 mobilizable multi-purpose cloning vectors derived from the *Escherichia coli* plasmids pK18 and pK19:
732 selection of defined deletions in the chromosome of *Corynebacterium glutamicum*. Gene 145, 69-73.

733 Schlüter, J.P., Reinkensmeier, J., Daschkey, S., Evguenieva-Hackenberg, E., Janssen, S., Jänicke,
734 S., Becker, J.D., Giegerich, R., Becker, A. (2010) A genome-wide survey of sRNAs in the symbiotic
735 nitrogen-fixing alpha-proteobacterium *Sinorhizobium meliloti.* BMC Genomics 2010 11, 245.

736 Schlüter, J.P., Czuppon, P., Schauer, O., Pfaffelhuber, P., McIntosh, M., and Becker, A. (2015)
737 Classification of phenotypic subpopulations in isogenic bacterial cultures by triple promoter probing at
738 single cell level. J Biotechnol. 198, 3-14.

739 Simon, R., Priefer, U., and Pühler, A. (1983) A broad host range mobilization system for in vivo genetic
740 engineering: transposon mutagenesis in Gram negative bacteria. Bio-Technology 1, 784-791.

741 Storz, G., Wolf, Y.I, Ramamurthi, K.S. (2014) Small proteins can no longer be ignored. Annu. Rev.
742 Biochem. 83, 753-777.

743 Terán, W., Krell, T., Ramos, J., L., and Gallegos, M., T. (2006) Effector-repressor interactions, binding
744 of a single effector molecule to the operator-bound TtgR homodimer mediates derepression. J. Biol
745 Chem. 281, 7102-7109.

746 Vitreschak, A.G., Lyubetskaya, E.V., Shirshin, M.A., Gelfand, M.S., and Lyubetsky, V.A. (2004)
747 Attenuation regulation of amino acid biosynthetic operons in proteobacteria: comparative genomics
748 analysis. FEMS Microbiol. Lett., 234, 357-370.

749 Waters, L.S., and Storz, G. (2009) Regulatory RNAs in bacteria. Cell 136, 615-628.

750 Weaver, J., Mohammad, F., Buskirk, A.R., Storz, G. (2019) Identifying Small Proteins by Ribosome
751 Profiling with Stalled Initiation Complexes. MBio. 10, pii: e02819-18.

752 Wickham H. (2016) ggplot2: Elegant Graphics for Data Analysis. Springer-Verlag New York,

753 Yanofsky C. (1981) Attenuation in the control of expression of bacterial operons. Nature 289, 751-758.

754 Yin, X., Wu Orr, M., Wang, H., Hobbs, E.C., Shabalina, S.A, and Storz G. (2019) The small protein
755 MgtS and small RNA MgrR modulate the PitA phosphate symporter to boost intracellular magnesium
756 levels. Mol. Microbiol 111, 131–144.

Zahn, K. (1996) Overexpression of an mRNA dependent on rare codons inhibits protein synthesis and cell growth. J. Bacteriol. 178, 2926-2933.

Zurawski, G., Elseviers, D., Stauffer, G.V., Yanofsky, C. (1978) Translational control of transcription termination at the attenuator of the *Escherichia coli* tryptophan operon. Proc. Natl. Acad. Sci. U. S A. 75, 5988-92.

Figure legends

Figure 1. The attenuator sRNA rnTrpL requires the leader peptide peTrpL and tetracycline for down-regulation of *rplUrpmA* mRNA. A) Schematic representation of the *S. meliloti trpLE(G)* locus. The *trpL* and *trpE(G)* ORFs (gray arrows), a RpoD-like promoter (gray rectangle), the transcription start site (flexed arrow) and the transcription terminator (hairpin) are depicted (according to Bae and Crawford, 1990). **B) C), D),** and **F)**, Log_2 fold changes (log_2FC) in *rpmA* mRNA levels determined by qRT-PCR are shown. Each graph contains data from three independent experiments, each performed in duplicates. Means with standard deviations (SD)s are indicated. **B)** Cultures of strain 2011 containing the indicated plasmids were analyzed. Bar C on the left, the *rpmA* level in the constitutively overexpressing strain 2011(pRK-rnTrpL) was compared to that in the EVC. All other bars show comparisons of the *rpmA* levels at the indicated times post induction (min IPTG) with the levels before induction. Presence of pRK4352 and Tc (20 µg/ml) is indicated. **C)** Cultures of strain 2011*ΔtrpL* containing the indicated plasmids and grown with Gm and Tc were analyzed. Changes in the *rpmA* levels 10 min post induction with IPTG were compared to those before induction. As shown below the graph, pSRKGm-rnTrpL leads to production of peTrpL (peptide) and the sRNA lacZ'-rnTrpL (sRNA), while pSRKGm-peTrpL leads to the production of the peptide only. **D)** Cultures of strain 2011*ΔtrpL* containing the indicated plasmids were analyzed. Induced production of peTrpL (peptide) and/or constitutive production of the rnTrpL derivative rnTrpL-AU1,2UA containing an inactivated *trpL* sORF (sRNA) is indicated. For other descriptions see panel C). **E)** Schematic representation of the experiment aiming to detect a short-term effect of Tc on *rpmA* expression in strain 2011*ΔtrpL* (pSRKGm-rnTrpL, pRK4352). The culture was grown first in medium with Gm and Tc. Then, the strain was grown for 4 h without Tc, IPTG was added and, 10 min later, Tc was also added. RNA was isolated at the indicated time points and the *rpmA* levels at the time points 10 and 20 min were compared to the level at the time point 0 (marked with arrows and asterisks). **F)** qRT-PCR analysis of changes in the *rpmA* level upon induction of lacZ'-rnTrpL transcription and/or exposure to Tc (see panel E and its description). Additionally, suitable controls were conducted: cultures were exposed to IPTG only, Tc only or to a combination of both compounds for the indicated times (min).

Figure 2. rnTrpL directly base-pairs with *rplU* and destabilizes the bicistronic *rplUrpmA* mRNA. A) Scheme of the *rplUrpmA* operon and the duplex structure predicted to be formed between *rplU* (mRNA) and rnTrpL (sRNA) (ΔG = -11.54 kcal/mol). **B)** Analysis of possible base-pairing interactions between lacZ'-rnTrpL and the fusion mRNA *rplUrpmA'::egfp* in strain 2011*ΔtrpL*. The plasmids used in this experiment are indicated. Cultures were grown with Gm and Tc, and fluorescence was measured

20 min after IPTG addition. The fluorescence of strain 2011*ΔtrpL* (pSRKGm-rplUrpmA'-egfp, pSRKTc) was set to 100 % and used for normalization. **C)** Determination of the half-lives of *rpmA* and (as a negative control) *rpoB* mRNA in strain 2011*ΔtrpL* (pSRKTc-rnTrpL) grown with Tc. 10 min after induction of rnTrpL transcription by IPTG, rifampicin (Rf) was added to stop cellular transcription. In parallel, a non-induced culture was treated with Rf. At the time points 0, 2, 4 and 6 min after Rf addition, RNA was isolated and analyzed by qRT-PCR. The mRNA level at time point 0 (before Rf addition) was set to 100%, the relative mRNA level values were plotted against the time, and the mRNA half-lives were calculated. Shown are the results from three independent transcription inhibition experiments. The qRT-PCRs reactions were performed in technical duplicates (means with SDs are indicated).

Figure 3. Tc-dependent CoIP of RNAs with 3×FLAG-peTrpL reveals a new target and antisense mechanism. A) The 3×FLAG-peTrpL retained functionality. Shown is a qRT-PCR analysis of changes in *rpmA* levels at 10 min post induction of peTrpL or 3×FLAG-peTrpL production in strains 2011(pSRKGm-peTrpL, pRK4352) and 2011(pSRKGm-3×FLAG-peTrpL, pRK4352), respectively. The cultures were grown with Gm and Tc. **B)** Enrichment of the indicated RNAs in the 3xFLAG-peTrpL CoIP samples, in comparison to the control, mock CoIP conducted with the peTrpL-containing lysate. One-step qRT-PCR was performed. The presence of Tc in the washing buffer is indicated. Shown are the results from three independent experiments, each performed in duplicates (means with SDs are indicated). **C)** RNAseq analysis revealed sense (se) and antisense (as) RNA of rnTrp, *rplUrpmA* and *smeR* in the 3×FLAG-peTrpL CoIP samples. Only RNA retained on the beads after washing with a Tc-containing buffer was sequenced, along with total RNA of strain 2011 grown under similar conditions, but without Gm and Tc. Shown is an IGB view of mapped cRNA reads. Annotated ORFs or transcripts are indicated.

Figure 4. peTrpL is involved in in the regulation of the multidrug efflux pump operon *smeABR*. **A)** qRT-PCR analysis of *smeR* in strain 2011*ΔtrpL* containing the indicated plasmids. Changes in the mRNA level 10 min post IPTG addition were determined. Co-transformation of pRK4352 and presence of Tc in the growth medium is also indicated (compare to Fig. 1B and 1C). **B)** *smeR* mRNA half-lives in 2011*ΔtrpL* (pSRKTc-rnTrpL) cultures induced or non-induced with IPTG for 10 min. For details, see Fig. 2C. **C)** qRT-PCR analysis of *smeA* mRNA. Time of peTrpL or rnTrpL induction by IPTG is indicated. For other details, see panel A). **D)** Co-transcription of *smeB* and *smeR* revealed by RT-PCR analysis of strain 2011*ΔtrpL,* 10 min after addition of 1.5 µg/ml Tc. **E)** qRT-PCR analysis of the reporter *egfp* mRNA, transcribed from plasmid pSUP-PasRegfp (see Fig. S1). The *egfp* mRNA level 10 min after addition of Tc (10 µg/ml) or one of the indicated antimicrobial substances (applied at subinhibitory concentrations: Em, 27 µg/ml, Cl, 9 µg/ml;Gs, 90 µg/ml; Rf, 3 µg/ml; Lt, 40 µg/ml, Km, 45 µg/ml) was compared to the level before addition. Data shown in the graphs were obtained from three independent experiments, each performed in technical duplicates (means and SDs are indicated). **F)** Current model for regulation of the *smeABR* operon. Exposure to SmeR-effectors relieves the *smeABR* repression by SmeR at the P_{se} promoter and leads to induction of asRNA transcription at the

836 P_{as} promoter. We postulate that the asRNA As-smeR and the peptide pTrpL are involved in the
837 accelerated decay of the *smeR* part of the *smeABR* transcript. This posttranscriptional regulation
838 results in increased production of the multidrug efflux pump SmeAB.

839

840 **Figure 5. The peptide peTrpL increases the resistance to multiple antimicrobial substances.**
841 Unless stated otherwise (see panel D), the deletion mutant 2011*ΔtrpL* was used for the experiments
842 shown in this figure. **A)** Zones of growth inhibition showing increased resistance to Tc upon induced
843 peTrpL production. Plasmids and presence of IPTG in the growth medium are indicated.
844 Representative plates are shown. **B)** Graphic representation of the results from the experiment shown
845 in A). **C)** and **D)** Graphs showing the OD_{600} values reached in 96-well plates at 14 hours post
846 inoculation at an OD_{600} of 0.1. In B, C) and D), data from three independent experiments were
847 included in the analysis. Shown are means and SDs. **C)** Ectopically expressed peTrpL increases the
848 bacterial resistance to Tc (0.2 µg/ml). Plasmids and presence of IPTG in the medium are indicated. **D)**
849 Strain 2011 grows better than the deletion mutant 2011*ΔtrpL* at a subinhibitory Tc concentration.
850 Strains and Tc concentrations are indicated. **E)** NileRed efflux assay for determination of the efflux
851 activity in the presence or absence of peTrpL production. Plasmids used and addition of IPTG are
852 indicated. 1.5 µg/ml Tc was added to the cultures. The NileRed dye generates a fluorescence signal
853 only if present in the cell. Fast decline of fluorescence over time correlates with high efflux pump
854 activity. Data of a representative experiment is shown. **F)** Production of peTrpL increases the MICs of
855 Cl, Em, Rf and Gs, but not of Km and Lt. Culture of strain 2011*ΔtrpL* (pSRKGm-peTrpL) was diluted to
856 an OD_{600} of 0.1 and grown for 60 h in 96-well plates. Concentrations of the antimicrobial compounds
857 used in the respective experiments are given above the panels. Presence of IPTG in the medium and
858 MICs are indicated on the left side. Shown is one representative result of three independent
859 experiments.

860

861 **Figure 6. Gene regulation in *trans* by two different, peTrpL-dependent pathways, and**
862 **generation of the sRNA rnTrpL in response to translation inhibition A)** Differential downregulation
863 of *rplUrpmA* and/or *smeR* in strain 2011 upon addition of the indicated antimicrobial compounds at
864 subinhibitory concentrations (see Fig. 4E). Changes in the levels of the indicated mRNAs 10 min after
865 exposure to the antimicrobials were determined by qRT-PCR. *trpE* was used as a negative control.
866 See also Fig. S5. **B)** Selective CoIP of 3×FLAG-peTrpL with *smeR* and/or *rplUrpmA*, the latter
867 together with rnTrpL, in the presence of different antimicrobial compounds, which were used at the
868 subinhibitory concentrations indicated in Fig. 4E. One half of the beads was washes with a buffer
869 containing Km, Cl or Gs, respectively, while the other half was washed with an antimicrobials-free
870 buffer. Only one of the negative controls (beads washed with buffer devoid of antimicrobials) is
871 presented. For details, see Fig 3B. The graphs show results from three independent experiments,
872 each performed in duplicates (means with SDs are indicated). **C)** Northern blot analysis of strain
873 2011*ΔtrpC* demonstrating the accumulation of rnTrpL as a consequence of transcription termination
874 upon exposure to Tc, under conditions of Trp insufficiency. A schematic representation of the
875 experiment is shown above the hybridization panels. 30 µg total RNA was loaded in each lane, except

for lane 1 in which 10 µg RNA was loaded. First, a probe directed against rnTrpL was used and, then, the membrane was re-hybridized with the 5S rRNA-specific probe (loading control). High Trp conditions, 20 µg/ml Trp in the minimal medium; Low Trp conditions, 2 µg/ml Trp in the minimal medium. Detected RNAs are indicated. **D)** Model for posttranscriptional regulation of *rplUrpmA* by rnTrpL generation at conditions of translation inhibition, even under conditions of Trp shortage. Based on our data, we propose that double-stranded RNA, base pairing between rnTrpL and *rplU*, peTrpL and the presence of a translation-inhibiting antibiotic, such as Tc or Cl, are involved in this posttranscriptional regulation.

Figure 7. Role of peTrpL in multiresistance is conserved in Rhizobiales despite high divergence in primary structure. A) Analysis of changes in the mRNA levels of *rpmA* and the respective *smeR* homolog upon overproduction of corresponding rnTrpL homologs in *A. tumefaciens* and *B. japonicum*. Plasmid pSRKGm-Atu-rnTrpL was used to induce Atu-rnTrpL production for 10 min. mRNA Levels after induction were compared to those before induction. Due to the lack of a suitable inducible system for *B. japonicum*, Bja-rnTrpL was overproduced constitutively from the chromosomally integrated, Tc-resistance-conferring plasmid pRJ-Bja-rnTrpL. **B)** The MIC of Tc for *A. tumefaciens* was increased upon induced overproduction of Atu-peTrpL from plasmid pSRKGm-Atu-peTrpL. **C)** Constitutive overproduction of Bja-peTrpL enables *B. japonicum* growth in a liquid medium containing 100 µg/ml Tc, while growth of the control strain containing the empty vector pRJ-MCS was inhibited at this Tc concentration. **D)** Sequence logos for peTrpL of the *Sinorhizobium, Agrobacterium* and *Bradyrhizobium* groups (see Fig. S7). **E)** Alanine scanning mutagenesis for analysis of functionally important residues in peTrpL of *S. meliloti*. Changes in the levels of *rpmA* and *smeR* were determined by qRT-PCR 10 min after addition of IPTG to induce the overproduction of peTrpL variants with the indicated aa exchanges in strain 2011. As EVC, bacteria cotransformed with pSRKGm and pRK4352 were used, while the strains used to overproduce wt peTrpL (or one of its variants with aa exchanges) were cotransformed with pSRKGm-peTrpL (or one of its mutated derivatives) and pRK4352. All cultures were grown with Gm and Tc. Shown are the results from three independent experiments, each performed in duplicates (means with SDs are indicated).

Figure 1

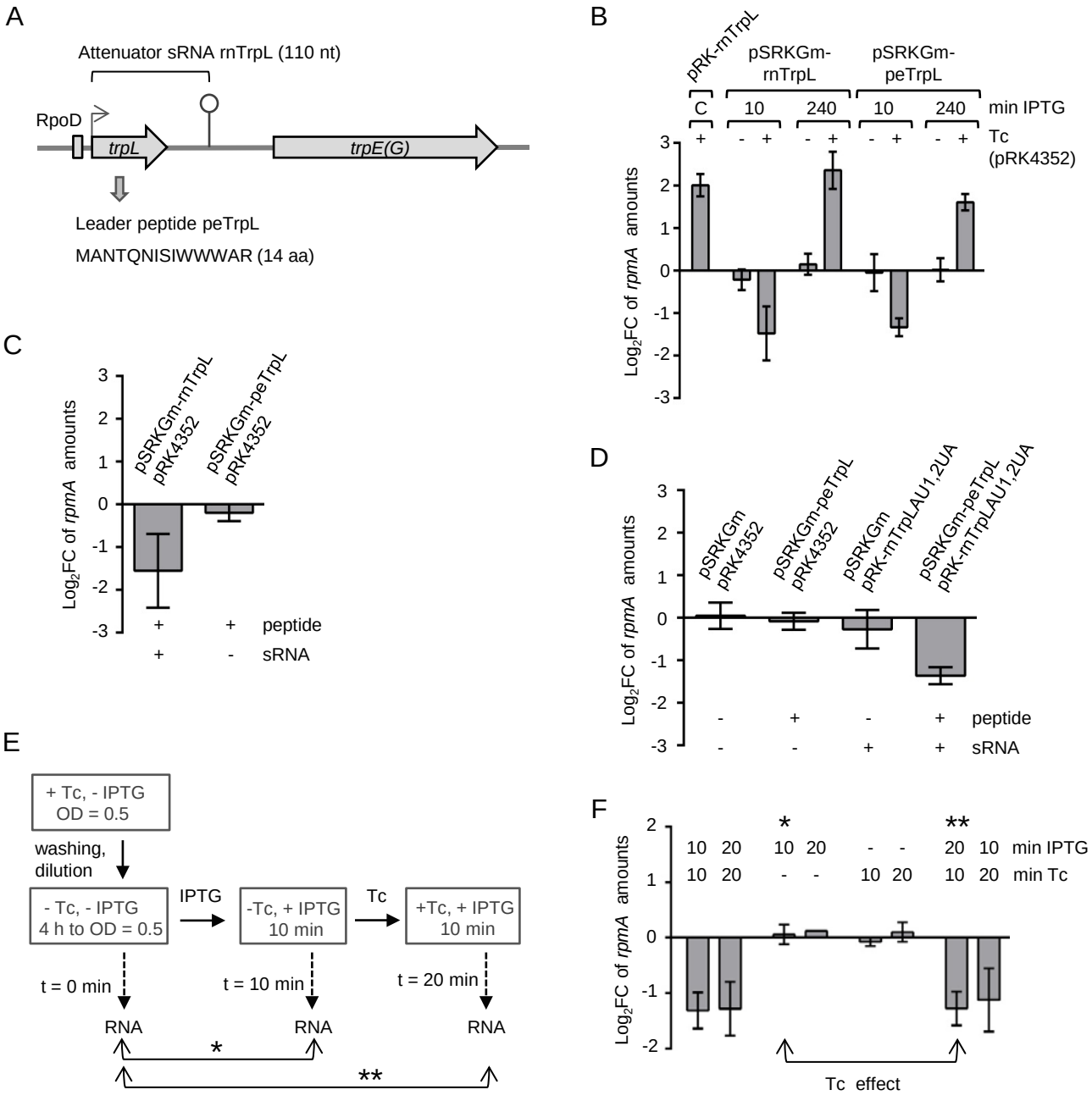
A
Attenuator sRNA rnTrpL (110 nt)
RpoD
trpL
trpE(G)
Leader peptide peTrpL
MANTQNISIWWWAR (14 aa)
B
pRK-rnTrpL
pSRKGm-rnTrpL
pSRKGm-peTrpL
C
10
240
10
240
min IPTG
Tc (pRK4352)
Log2FC of rpmA amounts
C
pSRKGm-rnTrpL pRK4352
pSRKGm-peTrpL pRK4352
peptide
sRNA
D
pSRKGm pRK4352
pSRKGm-peTrpL pRK4352
pSRKGm pRK-rnTrpLAU1,2UA
pSRKGm-peTrpL pRK-rnTrpLAU1,2UA
peptide
sRNA
E
+ Tc, - IPTG OD = 0.5
washing, dilution
- Tc, - IPTG 4 h to OD = 0.5
IPTG
-Tc, + IPTG 10 min
Tc
+Tc, + IPTG 10 min
t = 0 min
t = 10 min
t = 20 min
RNA
RNA
RNA
*
**
F
min IPTG
min Tc
Tc effect

Figure 2

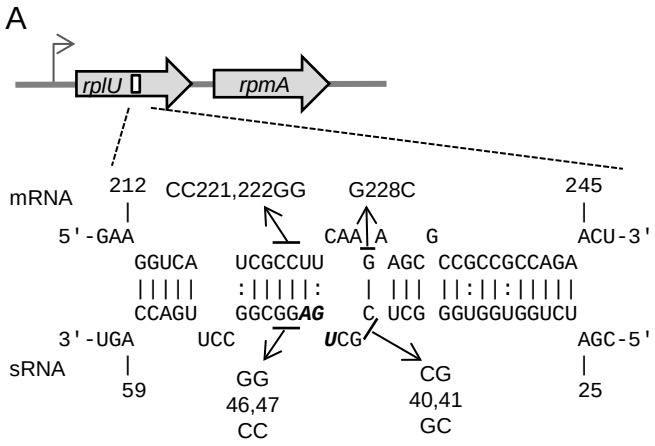
A
rplU
rpmA
mRNA
212
CC221,222GG
G228C
245
5'-GAA
CAA A G
ACU-3'
GGUCA UCGCCUU G AGC CCGCCGCCAGA
CCAGU GGCGGAG C UCG GGUGGUGGUCU
3'-UGA
UCC
UCG
AGC-5'
sRNA
59
GG
46,47
CC
CG
40,41
GC
25

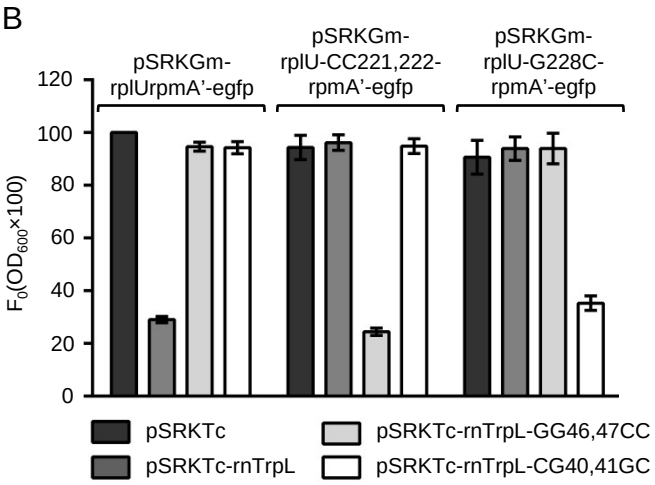
B
pSRKGm-rplURpmA'-egfp
pSRKGm-rplU-CC221,222-rpmA'-egfp
pSRKGm-rplU-G228C-rpmA'-egfp
F0(OD600×100)
120
100
80
60
40
20
0
pSRKTc
pSRKTc-rnTrpL
pSRKTc-rnTrpL-GG46,47CC
pSRKTc-rnTrpL-CG40,41GC

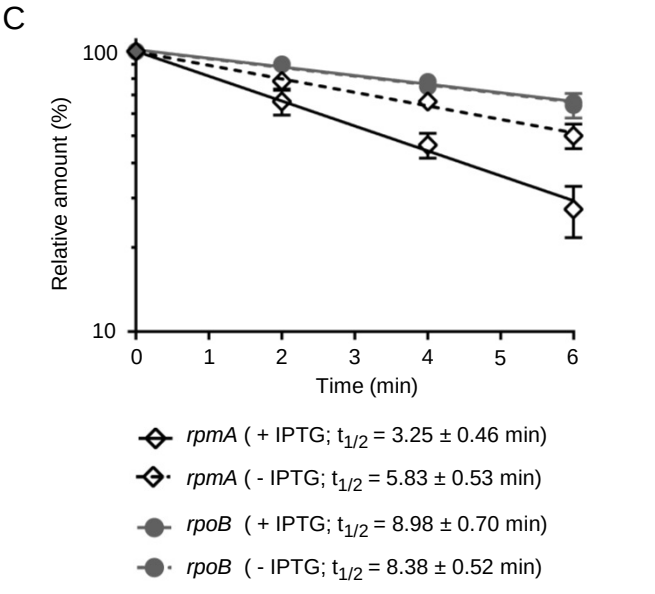
C
Relative amount (%)
100
10
0
1
2
3
4
5
6
Time (min)
rpmA (+ IPTG; t1/2 = 3.25 ± 0.46 min)
rpmA (- IPTG; t1/2 = 5.83 ± 0.53 min)
rpoB (+ IPTG; t1/2 = 8.98 ± 0.70 min)
rpoB (- IPTG; t1/2 = 8.38 ± 0.52 min)

Figure 3

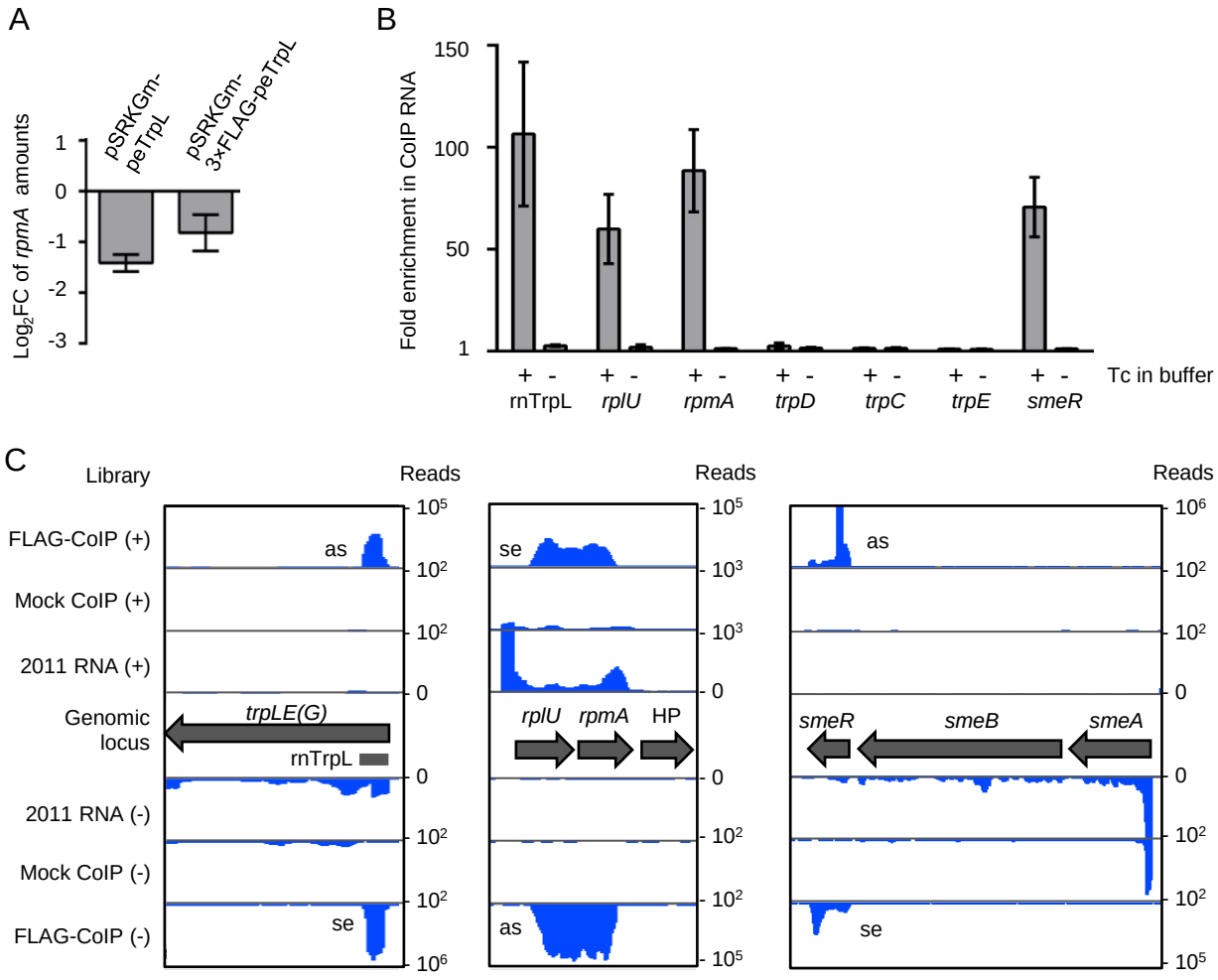
A
Log2FC of rpmA amounts
1
0
-1
-2
-3
pSRKGm-peTrpL
pSRKGm-3×FLAG-peTrpL
B
Fold enrichment in CoIP RNA
150
100
50
1
+ - + - + - + - + - + - + -
rnTrpL rplU rpmA trpD trpC trpE smeR
Tc in buffer
C
Library
Reads
FLAG-CoIP (+)
Mock CoIP (+)
2011 RNA (+)
Genomic locus
2011 RNA (-)
Mock CoIP (-)
FLAG-CoIP (-)
as
se
trpLE(G)
rnTrpL
rplU
rpmA
HP
smeR
smeB
smeA

Figure 4

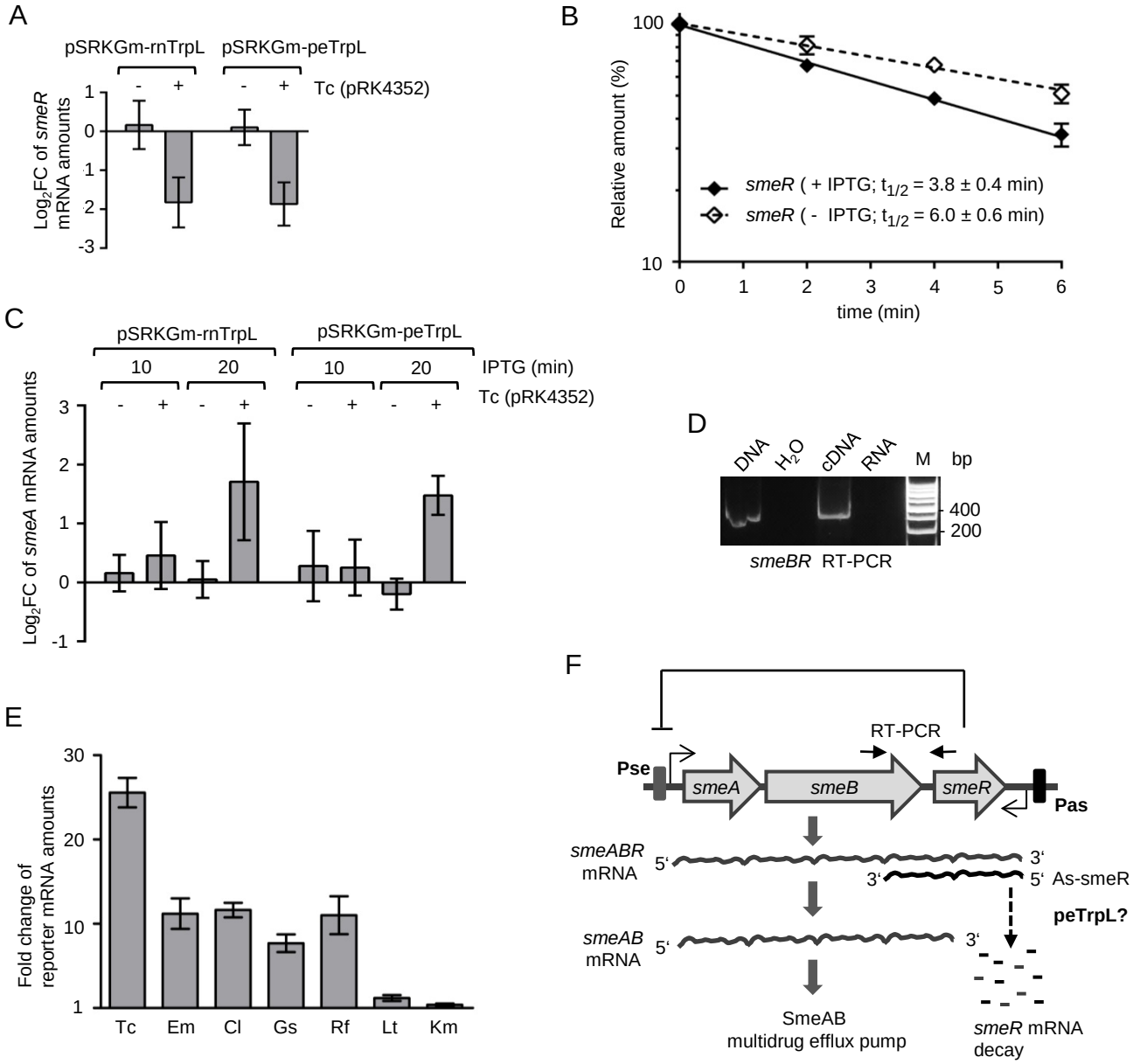
A
pSRKGm-rnTrpL
pSRKGm-peTrpL
- + - +
Tc (pRK4352)
Log2FC of smeR mRNA amounts
1
0
-1
-2
-3
B
100
10
Relative amount (%)
smeR (+ IPTG; t1/2 = 3.8 ± 0.4 min)
smeR (- IPTG; t1/2 = 6.0 ± 0.6 min)
0 1 2 3 4 5 6
time (min)
C
pSRKGm-rnTrpL
pSRKGm-peTrpL
10 20 10 20
IPTG (min)
- + - + - + - +
Tc (pRK4352)
Log2FC of smeA mRNA amounts
3
2
1
0
-1
D
DNA
H2O
cDNA
RNA
M
bp
400
200
smeBR RT-PCR
E
Fold change of reporter mRNA amounts
30
20
10
1
Tc Em Cl Gs Rf Lt Km
F
RT-PCR
Pse
smeA
smeB
smeR
Pas
smeABR mRNA
5‘
3‘
3‘
5‘
As-smeR
peTrpL?
smeAB mRNA
5‘
3‘
SmeAB multidrug efflux pump
smeR mRNA decay

Figure 5

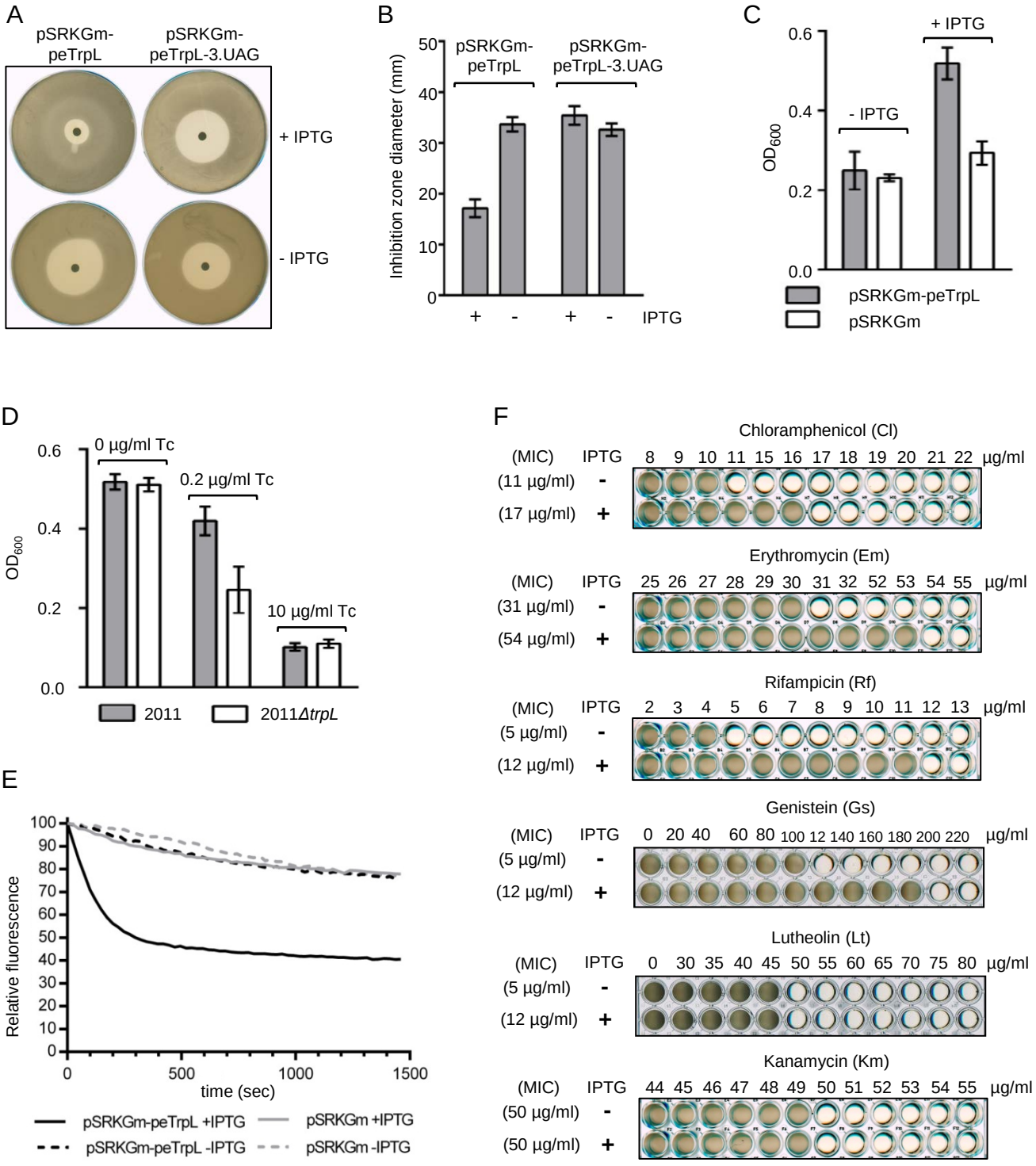
A
pSRKGm-peTrpL
pSRKGm-peTrpL-3.UAG
+ IPTG
- IPTG
B
Inhibition zone diameter (mm)
pSRKGm-peTrpL
pSRKGm-peTrpL-3.UAG
IPTG
C
+ IPTG
- IPTG
OD600
pSRKGm-peTrpL
pSRKGm
D
0 μg/ml Tc
0.2 μg/ml Tc
10 μg/ml Tc
OD600
2011
2011ΔtrpL
E
Relative fluorescence
time (sec)
pSRKGm-peTrpL +IPTG
pSRKGm +IPTG
pSRKGm-peTrpL -IPTG
pSRKGm -IPTG
F
Chloramphenicol (Cl)
(MIC) IPTG 8 9 10 11 15 16 17 18 19 20 21 22 μg/ml
(11 μg/ml) -
(17 μg/ml) +
Erythromycin (Em)
(MIC) IPTG 25 26 27 28 29 30 31 32 52 53 54 55 μg/ml
(31 μg/ml) -
(54 μg/ml) +
Rifampicin (Rf)
(MIC) IPTG 2 3 4 5 6 7 8 9 10 11 12 13 μg/ml
(5 μg/ml) -
(12 μg/ml) +
Genistein (Gs)
(MIC) IPTG 0 20 40 60 80 100 12 140 160 180 200 220 μg/ml
(5 μg/ml) -
(12 μg/ml) +
Lutheolin (Lt)
(MIC) IPTG 0 30 35 40 45 50 55 60 65 70 75 80 μg/ml
(5 μg/ml) -
(12 μg/ml) +
Kanamycin (Km)
(MIC) IPTG 44 45 46 47 48 49 50 51 52 53 54 55 μg/ml
(50 μg/ml) -
(50 μg/ml) +

Figure 6

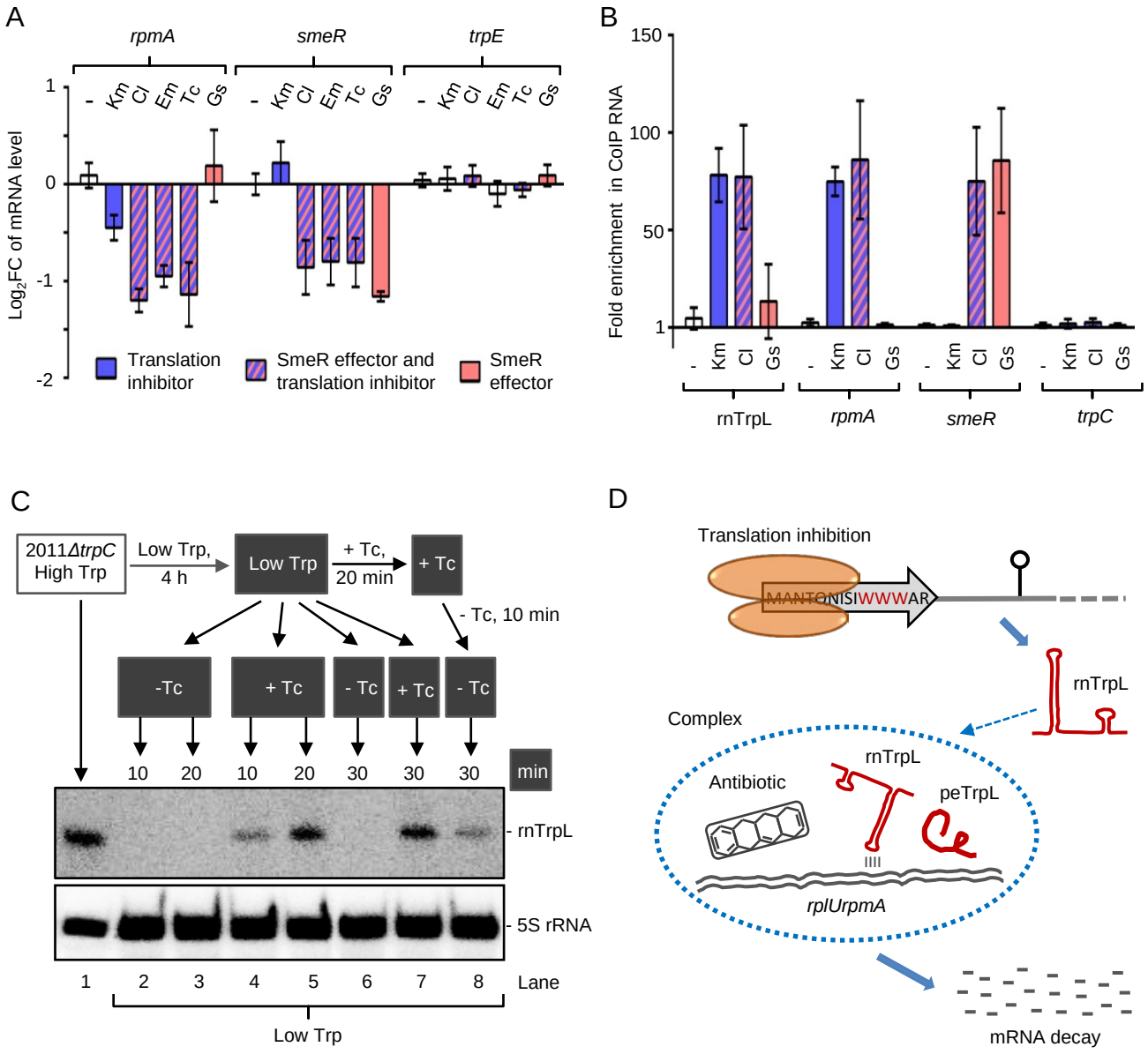
A
rpmA
smeR
trpE
- Km Cl Em Tc Gs
Log2FC of mRNA level
1
0
-1
-2
Translation inhibitor
SmeR effector and translation inhibitor
SmeR effector
B
Fold enrichment in CoIP RNA
150
100
50
1
- Km Cl Gs
rnTrpL
rpmA
smeR
trpC
C
2011ΔtrpC High Trp
Low Trp, 4 h
Low Trp
+ Tc, 20 min
+ Tc
- Tc, 10 min
-Tc
+ Tc
- Tc
+ Tc
- Tc
10 20 10 20 30 30 30 min
- rnTrpL
- 5S rRNA
1 2 3 4 5 6 7 8 Lane
Low Trp
D
Translation inhibition
MANTONISIWWWAR
rnTrpL
Complex
rnTrpL
Antibiotic
peTrpL
rplUrpmA
mRNA decay

Figure 7

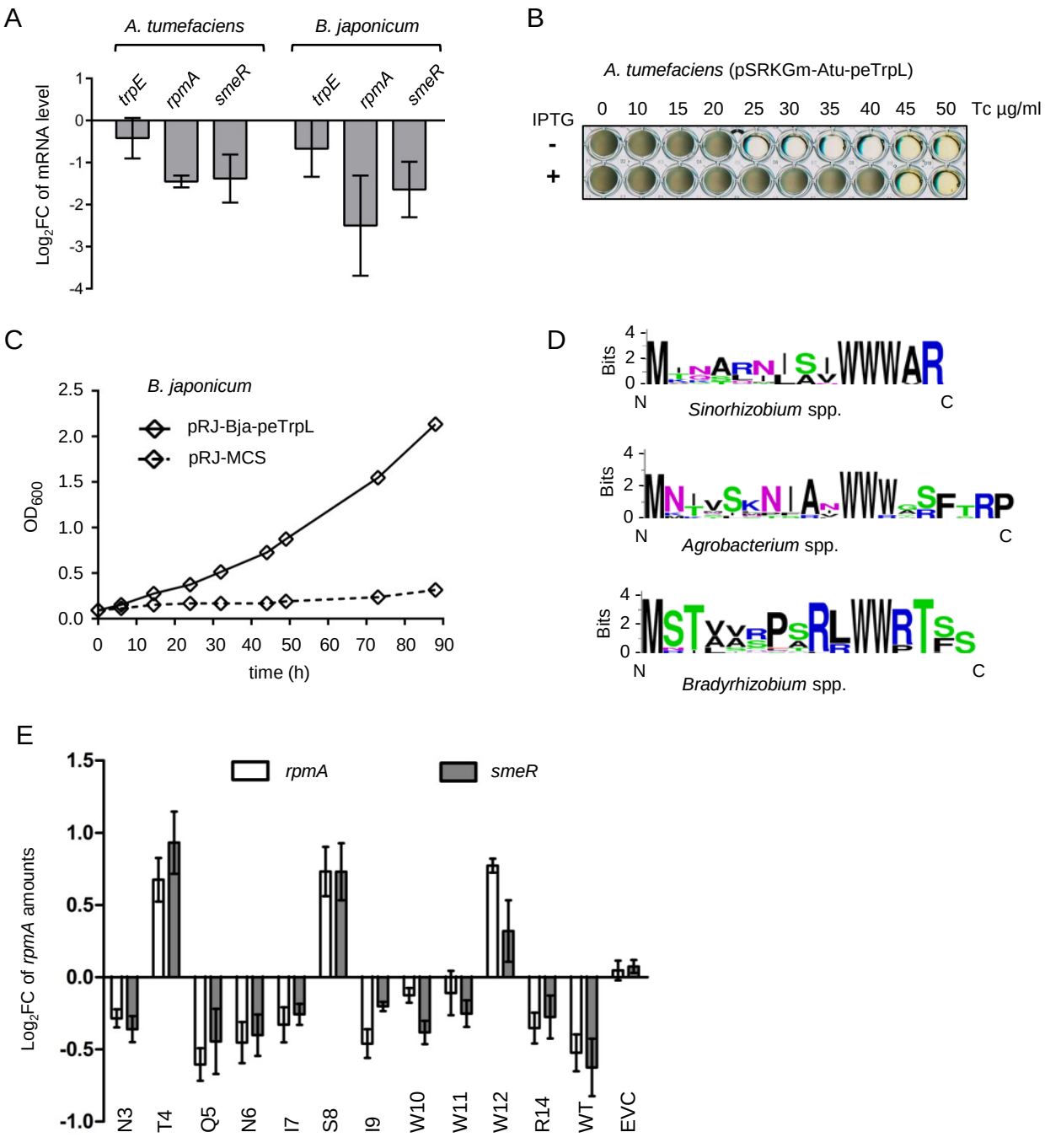
A
A. tumefaciens
B. japonicum
trpE
rpmA
smeR
trpE
rpmA
smeR
Log2FC of mRNA level
1
0
-1
-2
-3
-4
B
A. tumefaciens (pSRKGm-Atu-peTrpL)
IPTG
0 10 15 20 25 30 35 40 45 50 Tc µg/ml
-
+
C
B. japonicum
pRJ-Bja-peTrpL
pRJ-MCS
OD600
2.5
2.0
1.5
1.0
0.5
0.0
0 10 20 30 40 50 60 70 80 90
time (h)
D
Bits
4
2
0
N
C
Sinorhizobium spp.
Agrobacterium spp.
Bradyrhizobium spp.
E
rpmA
smeR
Log2FC of rpmA amounts
1.5
1.0
0.5
0.0
-0.5
-1.0
N3
T4
Q5
N6
I7
S8
I9
W10
W11
W12
R14
WT
EVC